Marine Ecosystems

SOUTH AUSTRALIAN RESEARCH & DEVELOPMENT INSTITUTE
PIRSA

Aquaculture Environmental Monitoring Program: 2015-2019

Jason E. Tanner, Mark Doubell, John Middleton, Paul van Ruth and Charles James

SARDI Publication No. F2019/000334-1
SARDI Research Report Series No. 1053

SARDI Aquatics Sciences
PO Box 120 Henley Beach SA 5022

March 2020

Report prepared for PIRSA Fisheries and Aquaculture

SOUTH AUSTRALIA

Government of South Australia
Primary Industries and Regions SA

SARDI
SOUTH AUSTRALIAN RESEARCH AND DEVELOPMENT INSTITUTE

Aquaculture Environmental Monitoring Program: 2015-2019

Report prepared for PIRSA Fisheries and Aquaculture

Jason E. Tanner, Mark Doubell, Paul van Ruth, Charles James and John Middleton

SARDI Publication No. F2019/000334-1
SARDI Research Report Series No. 1053

March 2020

This publication may be cited as:

Tanner, JE, M Doubell, P van Ruth, C James and J Middleton (2020). Aquaculture Environmental Monitoring Program: 2015-2019. South Australian Research and Development Institute (Aquatic Sciences), Adelaide. SARDI Publication No. F2019/000334-1. SARDI Research Report Series No. 1053. 67pp.

South Australian Research and Development Institute
SARDI Aquatic Sciences
2 Hamra Avenue
West Beach SA 5024
Telephone: (08) 8207 5400
Facsimile: (08) 8207 5415
http://www.pir.sa.gov.au/research

DISCLAIMER

The authors warrant that they have taken all reasonable care in producing this report. The report has been through the SARDI internal review process, and has been formally approved for release by the Research Director, Aquatic Sciences. Although all reasonable efforts have been made to ensure quality, SARDI does not warrant that the information in this report is free from errors or omissions. SARDI and its employees do not warrant or make any representation regarding the use, or results of the use, of the information contained herein as regards to its correctness, accuracy, reliability and currency or otherwise. SARDI and its employees expressly disclaim all liability or responsibility to any person using the information or advice. Use of the information and data contained in this report is at the user's sole risk. If users rely on the information they are responsible for ensuring by independent verification its accuracy, currency or completeness. The SARDI Report Series is an Administrative Report Series which has not been reviewed outside the department and is not considered peer-reviewed literature. Material presented in these Administrative Reports may later be published in formal peer-reviewed scientific literature.

SARDI Publication No. F2019/000334-1
SARDI Research Report Series No. 1053

Author(s):	Jason E. Tanner, Mark Doubell, Paul van Ruth, Charles James and John Middleton
Reviewer(s):	Kathryn Wiltshire and Gretchen Grammer
Approved by:	A/Prof Tim Ward Science Leader, Marine Ecosystems
Signed:	
Date:	24 March 2020
Distribution:	PIRSA Fisheries & Aquaculture, SAASC Library, Parliamentary Library, State Library and National Library
Circulation:	Public Domain

TABLE OF CONTENTS

LIST OF FIGURES

LIST OF TABLES

ACKNOWLEDGEMENTS

The authors would like to acknowledge the support of PIRSA Fisheries and Aquaculture, Australian Southern Bluefin Tuna Industry Association Inc. and Clean Seas Aquaculture Growout Pty Ltd. We thank Paul Malthouse, Leo Mantilla, Ian Moody and the crew of the *RV Ngerin* for undertaking the field component of this project. Leo Mantilla sorted and identified the infauna. Ian Moody counted and identified the zooplankton. Paul Malthouse prepared and led the pelagic field surveys. SARDI oceanographic modelling is provided through the eSA-Marine collaboration (https://pir.sa.gov.au/research/esa_marine) in partnership with the Bureau of Meteorology and is supported by the Fisheries Research and Development Corporation (FRDC) and the Australian Southern Bluefin Tuna Industry Association. Thank you also to Kathryn Wiltshire and Gretchen Grammer for providing constructive comments on the manuscript.

EXECUTIVE SUMMARY

An independent review of the environmental monitoring program for aquaculture in South Australia recommended the development of regional and zone scale environmental monitoring, as well as site-scale auditing of industry practices. Consequently, SARDI undertook a 4-year environmental monitoring program from 2015/16 to 2018/19 for the tuna and other finfish sectors, which encompassed both regional and zone scale measurements and monitoring of benthic and pelagic ecosystems, which we report on here. 'Tuna' and 'Other Finfish' aquaculture is currently most active in two zones, the Boston Bay aquaculture zone and the Lincoln aquaculture zone.

This Aquaculture Environmental Monitoring Program (AEMP) is divided into two components: 1. pelagic and oceanographic monitoring, including an update of the coupled hydrodynamic-biogeochemical model and related carrying capacity software, 'CarCap', used by PIRSA Fisheries and Aquaculture for aquaculture planning and management; 2. a benthic component that looks at regional effects on infauna. The benthic component also included a temporal analysis of previous tuna environmental monitoring program (TEMP) and finfish environmental monitoring program (FEMP) data, which failed to detect any effects of aquaculture, although it did show larger-scale spatial differences in Spencer Gulf, as well as temporal change in the assemblage, which appeared to be cyclic in nature.

The objectives of the pelagic and oceanography component of the program are to:

- Determine baseline values and the extent of environmental, chemical and biological variability in relation to water quality and planktonic ecosystem composition to assess past (where available) and future changes in the trophic state of the Boston Bay and Lincoln (inner sector) aquaculture zones and connected coastal systems.
- Use the collected data and aquaculture feed inputs to update and validate the coupled hydrodynamic-biogeochemical for Spencer Gulf, and provide an update of the model via the 'CarCap' software to PIRSA to assist in regional aquaculture planning and management.

The objectives of the benthic component of the program reported here are to:

- Determine if there is any regional scale effect of tuna and finfish aquaculture on infauna in and around the Boston Bay and Lincoln (inner sector) aquaculture zones.

- Determine if the infaunal assemblages show any change between 2016 and 2018, the two years in which sampling was undertaken.

The pelagic environment and oceanography monitoring detected significant spatial and temporal variations in the physical environment, circulation, water quality and planktonic ecosystem composition. In comparison to previous studies, several water quality and phytoplankton based indicators show inshore sites within Boston and Louth Bay's differ significantly from offshore sites. Trends for several indicators collectively indicate the differences observed at inshore sites are consistent with impacts expected from anthropogenic nutrient enrichment. These indicators were nutrients, chlorophyll *a*, phytoplankton abundance and community composition, harmful algal bloom (HAB) species and frequency, and planktonic community size structure and composition. The trends are supported by oceanographic modelling, which provides a greater understanding of natural and anthropogenic nutrient supply, connectivity and dispersal in the region and at the scale of the gulf. The coupled hydrodynamic-biogeochemical model for Spencer Gulf is updated for the years 2016, 2017 and 2018. This model includes nutrients supplied to the gulf through natural exchange with shelf waters and anthropogenic nutrients sourced from aquaculture and other industries. To assist in regional aquaculture planning and management, the updated model outputs are provided to PIRSA Fisheries and Aquaculture via the 'CarCap' software.

The regular monitoring of planktonic assemblages and water quality is a new component of environmental monitoring program for the tuna and marine finfish aquaculture industries in South Australia. Importantly, the results provide enough sensitivity to indicate that aquaculture is having a detectable impact on water quality and trophic state at the inshore sites within Boston and Louth Bay's, as well as providing a baseline and a set of multiple, complimentary indicators for explaining future changes, natural or anthropogenic. It is recommended that pelagic monitoring and modeling be continued given that the complex relationships between the physical environment, nutrient supply and the planktonic ecosystem response require more than six data points to be properly understood (two sampling events per year, one in in summer and one in autumn).

Both spatial and temporal variation were detected in the infaunal assemblages in the Boston Bay and Lincoln (inner) aquaculture zones, but there was no indication that aquaculture had a significant impact on the infauna. Instead, there were differences between groups of reference sites in both zones, consistent with a north-south gradient in infaunal assemblages. A similar

result was found in an earlier combined analysis of tuna and finfish environmental monitoring program data that included all samples collected between 2005 and 2014.

Assessment of infaunal assemblages has been a key component of environmental monitoring for the tuna and marine finfish aquaculture industries in South Australia since ~2001. During this time, there has been no indication that aquaculture has had any detectable impact on these organisms. Consequently, under current management and operational arrangements, and with an allowable zone of impact extending to 150m, continued monitoring is unlikely to detect any impacts. It is thus recommended that infaunal monitoring be scaled back, and only be undertaken on the order of once every five years. It should be stressed that this recommendation only holds under current arrangements. If there is appreciable change in the manner or location of farming, then infaunal monitoring will still likely be required on a more frequent basis.

Given the indications that aquaculture may be having some effect on the ecosystem, the 2019-2023 AEMP will undertake more detailed investigations into how these nutrients might be affecting seagrasses in the region. These studies will enable us to determine whether or not aquaculture is having a sustained negative impact on a key ecosystem asset.

Keywords: Infauna, oceanography, nutrients, phytoplankton, hydrodynamic modelling, biogeochemical modelling

1. INTRODUCTION

1.1. Background

Aquaculture is an important economic activity in Australia, with a gross production value of $1.3 billion in 2016/17 (Mobsby 2018). Key marine species include Pacific oyster *Crassostrea gigas*, Atlantic salmon *Salmo salar*, southern bluefin tuna (SBT) *Thunnus maccoyii*, ocean rainbow trout *Oncorhynchus mykiss* and yellowtail kingfish (YTK) *Seriola lalandi* (Mobsby 2018). In 2016/17, the aquaculture industry in South Australia had a total production value of $230.52 million, of which $115 million was for SBT and $27.09 million for other marine finfish (Econsearch 2018). Total aquaculture production declined 6% by weight and 8% by value over the previous year.

The management of the finfish aquaculture industry, which includes SBT and YTK, is based on the principles of ecologically sustainable development (ESD) enshrined in the South Australian *Aquaculture Act 2001*. One aspect of ESD is to ensure that aquaculture operations do not deleteriously and irreversibly change the marine environment. To assess compliance with this requirement, aquaculture licensees are legally required under the South Australian *Aquaculture Act 2001* and the *Aquaculture Regulations 2016* to undertake an Environmental Monitoring Program.

The Tuna Environmental Monitoring Program (TEMP) and Finfish Aquaculture Environmental Monitoring Program (FEMP) were both farm-site compliance-based monitoring programs using a system developed by South Australian Research and Development Institute (SARDI), comprising DNA-based assays using quantitative real-time PCR (qPCR) for selected benthic marine organisms in sediment, and an Environmental Compliance Scorecard system for analysing and presenting the results from the assays (Loo et al. 2006, Loo et al. 2010). This system was implemented for the TEMP in 2005 (e.g. Loo and Giblot-Ducray 2015) and the FEMP in 2009 (e.g. Loo and Giblot-Ducray 2014), and continued to 2014 and 2013, respectively.

An independent review of the environmental monitoring program for aquaculture in South Australia recommended the development of regional and zone scale environmental monitoring, as well as site-scale auditing of industry practices. These recommendations were based on the recognition that a significant portion of finfish aquaculture waste products occur ultimately as dissolved nutrients whose cumulative impacts are likely to be realised at some distance from

their source. Consequently, SARDI undertook a 4-year environmental monitoring program from 2015/16 to 2018/19 that encompassed both regional and zone scale measurements and monitoring of benthic and pelagic ecosystems, which we report on here.

'Tuna' and 'Other Finfish' aquaculture is currently most active in two zones, the Boston Bay aquaculture zone and the Lincoln aquaculture zone. The Lincoln aquaculture zone comprises the Lincoln (inner) sector, located east of Boston Island and the Lincoln (outer) sector, located south-east of Sir Joseph Banks group of islands (Figure 1.1). Most of the active leases for 'Tuna' (SBT) are currently operating in the southern part of the Lincoln (inner) sector, while active leases for 'Other Finfish' (YTK) are operating in the Boston Bay aquaculture zone. As only one SBT lease was operating in the Lincoln (outer) sector, the scope of this study did not include this region.

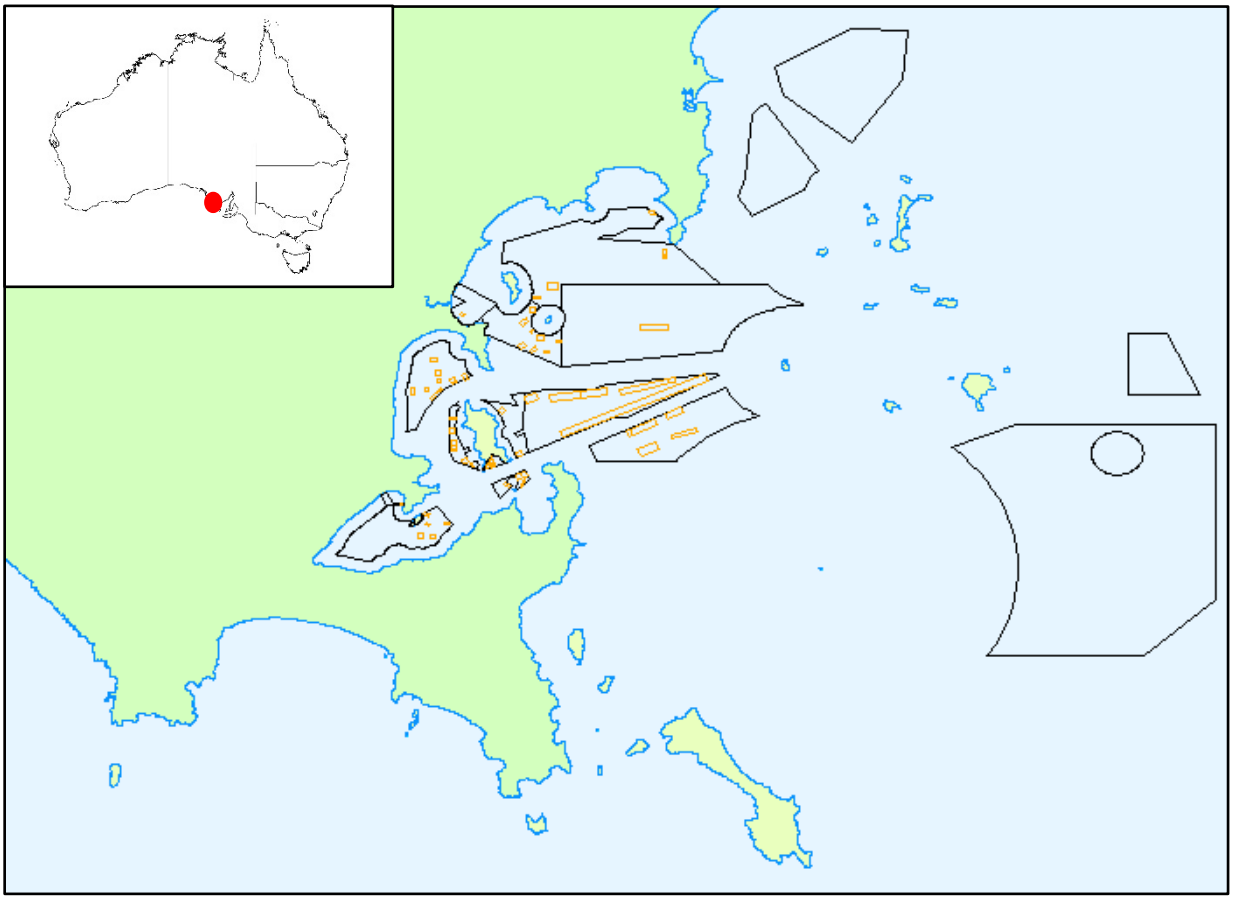

Figure 1.1: Map of the Boston Bay region showing the location of aquaculture zones (black polygons) and active aquaculture leases in 2018 (orange polygons). Note that not all zones and leases are for finfish, with some being for shellfish. Inset shows the location of the Boston Bay region (red dot).

The monitoring program described here was designed to assess key ecosystem groups to better understand the localised and cumulative impacts of finfish aquaculture in the Lincoln aquaculture zone (inner sector) and Boston Bay aquaculture zone. It is divided into two components: 1. a pelagic and oceanographic monitoring component that also includes an update of the coupled hydrodynamic-biogeochemical model and related CarCap software (Middleton et al. 2013) used by PIRSA F&A for aquaculture planning and management; 2. a benthic ecosystem component that looks at regional effects on infauna. The benthic component also included a temporal analysis of previous TEMP and FEMP data, which failed to detect any effects of aquaculture, although it did show larger-scale spatial differences in Spencer Gulf, as well as temporal change in the assemblage, which appeared to be cyclic in nature (Tanner et al. 2017).

This program is in line with recommendations from the independent review, and covers the minimum requirements to ensure baseline scientific rigour in the results. The combined monitoring and modelling program (as well as outcomes from other research projects, e.g. seagrass condition) will assist in the refinement of any future monitoring programs.

1.2. Objectives

The objectives of the pelagic and oceanography component of the program are to:

- Determine baseline values and the extent of environmental, chemical and biological variability in relation to water quality and planktonic ecosystem composition in order to assess past (where available) and future changes in the trophic state of the Boston Bay and Lincoln (inner sector) aquaculture zones and connected coastal systems.
- Use the collected data and aquaculture feed inputs to update and validate the coupled hydrodynamic-biogeochemical for Spencer Gulf, and provide an update of the model via the ‘CarCap’ software to PIRSA to assist in regional aquaculture planning and management.

The objectives of the benthic component of the program reported here are to:

- Determine if there is any regional scale effect of tuna and finfish aquaculture on infauna in and around the Boston Bay and Lincoln (inner sector) aquaculture zones.
- Determine if the infaunal assemblages show any change between 2016 and 2018, the two years in which sampling was undertaken.

2. PELAGIC AND OCEANOGRAPHY COMPONENT

2.1. Introduction

The water quality and health of coastal marine systems are vulnerable to nutrient over-enrichment, which can lead to an increase in organic (i.e. carbon) matter production (Nixon 1995). Natural drivers which influence nutrient supply in Spencer Gulf include climate driven changes, which determine the exchange of waters between the shelf and gulf (Middleton et al. 2013) and processes which affect the remineralization and resuspension of nutrient-rich sediment particulate matter (Tanner and Volkman 2009). Anthropogenic nutrient sources include those originating from finfish aquaculture and other industries (Gaylard 2014). Globally, the impacts of eutrophication are well documented (Howarth 2008, Glibert 2017) with common symptoms including increases in phytoplankton biomass, changes in plankton community composition and food-web structure, increased harmful algal bloom frequency, habitat degradation and a loss of biodiversity.

Since plankton form the base of the marine food web, their biomass and composition are useful indicators to manage coastal waterways (Cloern 2001, Paerl et al. 2003, Suthers et al. 2019). This is because plankton contain the majority of the pelagic biomass, and are responsible for the bulk of primary production and nutrient cycling. Ultimately, the productivity of the lower trophic (planktonic) ecosystem is influenced by the physical and chemical conditions which control nutrient supply, and is a function of plankton community composition. Hence, the size structure of plankton assemblages is a key characteristic which influences ecosystem productivity, dynamics and stability (Glibert 2017, Suthers et al. 2019, Van Meerssche and Pinckney 2019). For example, phytoplankton form the base of marine food webs and are responsible for primary production. Phytoplankton cell sizes span several orders of magnitude (picophytoplankton 0.2-2 µm, nanophytoplankton 2-20 µm, microphytoplankton >200 µm), and strongly influence the uptake of dissolved nutrients from the environment. Bacteria and zooplankton are important heterotrophic organisms which play key roles in food web dynamics. Bacteria are the principal organisms involved in nutrient recycling via the microbial loop (Azam and Malfatti 2007). Zooplankton grazers provide the main pathway from plankton to fish (Suthers et al. 2019).

This chapter provides a baseline description of water quality variables and the basic structural properties of plankton assemblages, including their temporal and spatial variability and relation to environmental forcing, for several sites in and around the Boston Bay and Lincoln aquaculture zones. Where possible, comparisons to historical observations made by Tanner and Volkman (2009) and Middleton et al. (2013) are provided to assess if any changes have taken place. The baseline measures reported here include several indicators based on planktonic ecosystem composition, which can be used to detect future changes in the trophic state of the coastal waters surrounding the Boston Bay and Lincoln aquaculture zones. An update of the coupled hydrodynamic-biogeochemical for Spencer Gulf (Middleton et al. 2013) is undertaken to better understand the influence of the physical environment on nutrient supply and the planktonic ecosystem response, as well as the connectivity and cumulative impact of anthropogenic nutrient loads at local and regional scales.

2.2. Methods

Field Surveys

The Pelagic Monitoring program comprises five sampling sites (Figure 2.1); one within the zone where tuna farming exists (LFZ), one just outside the Boston Bay aquaculture zone (BXZ), one to the south of the tuna farming zone used as a control site (LRS), and sites in Louth Bay (BRN) and to the north of the tuna farming aquaculture zone (LRN), where circulation models predict the cumulative transport of nutrients sourced from SBT and YTK aquaculture (Middleton et al. 2013, Doubell et al. 2015). Monitoring focused on two seasons; summer and autumn. Summer sampling was undertaken in January, as the annual cycle of nutrient loads from aquaculture begins to ramp up (see Figure 2.12) and connectivity with the shelf is restricted by the establishment of a summertime front across the entrance to the gulf (Petrusevics 1993). Autumn sampling was undertaken in May, when nitrogen loads from aquaculture are greatest, the annual flushing of the gulf draws an inflow of water from the shelf into and along the western side of the gulf (Lennon et al. 1987, Nunes Vaz et al. 1990), and phytoplankton productivity and biomass peaks (Tanner and Volkman 2009, Middleton et al. 2013).

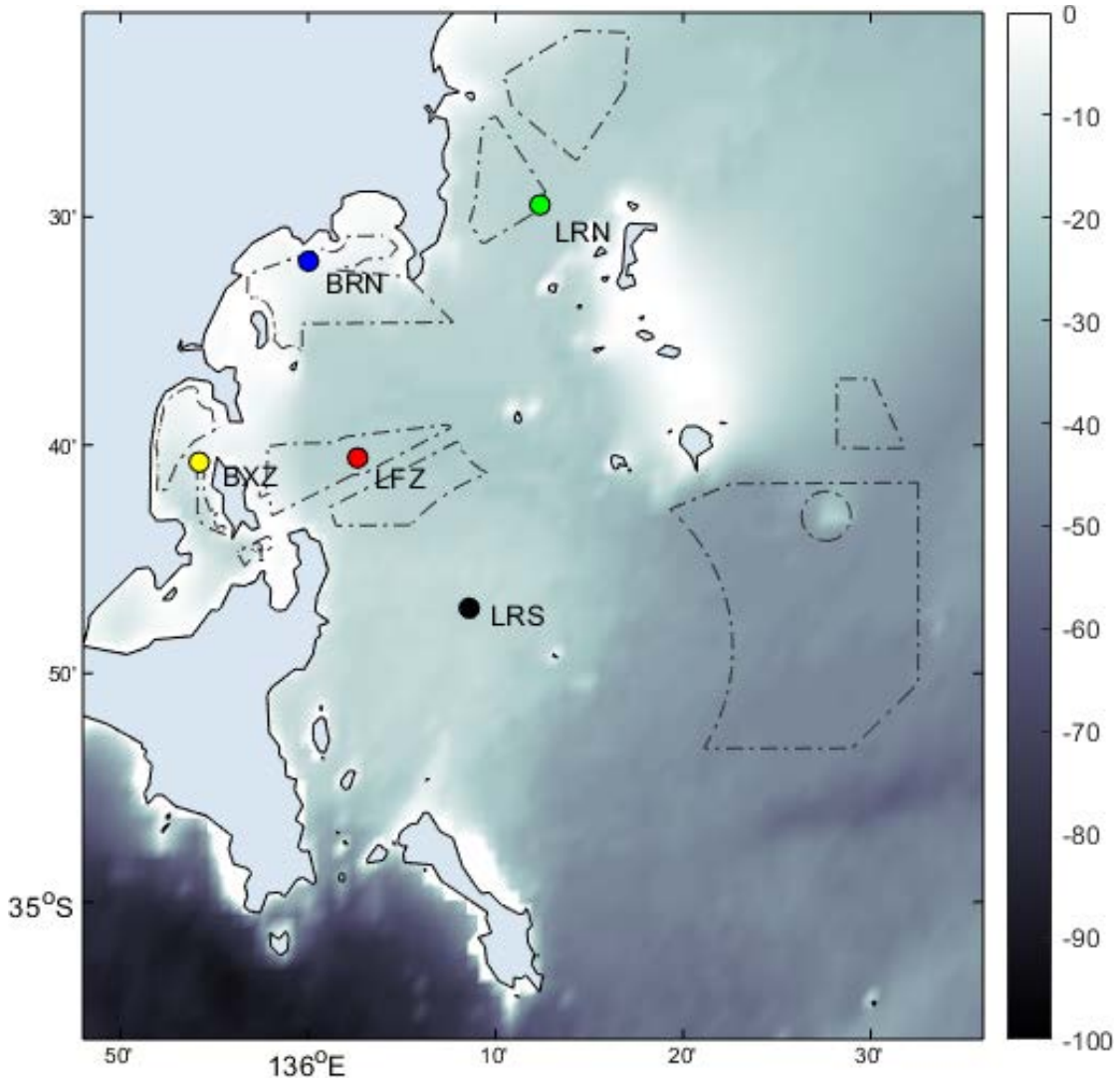

Figure 2.1: Bathymetric map of the lower Eyre Peninsula region showing the location of aquaculture zones and sampling sites. The mooring was located at the site LRS (black marker). The side bar shows the depth scale (m).

Field sampling was carried out in January and May 2016, 2017 and 2018. An oceanographic mooring was deployed at the LRS site in January and collected in May of each year. The mooring was positioned in a relatively flat area to the south of the Lincoln aquaculture zone help resolve the inflows that affect the aquaculture region farther north and to the west. The mooring contained an RDI Acoustic Doppler Current Profiler and NXIC CTD (conductivity-temperature-depth), and provided hourly measurements of currents throughout the water column and near bottom measures of temperature and salinity. Coincident with mooring deployment and retrieval, vertical profiles of temperature, salinity and in vivo chlorophyll a (chl a) fluorescence were acquired with a SeaBird SBE 19plus CTD equipped with a WetLabs ECO FL fluorometer. Following CTD

profiling at all sites, vertical net tows for zooplankton abundances using 64 and 150 µm mesh sizes were undertaken. Near surface and bottom water samples were then collected using a Niskin bottle and combined. From this the following sub-samples were taken:

- triplicate 50 mL samples for macro-nutrient analysis including; oxides of nitrogen (NO_x), ammonia (NH_4^+), phosphorus (PO_4^{3-}) and silica (SiO_2)
- triplicate 1 mL samples for the flow cytometric determination of bacteria, picophytoplankton and nanophytoplankton abundances
- triplicate 2 L samples for extracted chl a concentration
- a single 2 L sample for phytoplankton pigment composition using High Pressure Liquid Chromatography (HPLC)
- triplicate 500 mL samples for total suspended solid (TSS) concentration
- a single 1 L sample for microphytoplankton identification and abundance via light microscopy.

Analytical methods

For macro-nutrient analysis, 100 ml of water was filtered through a 0.45 µm filter, frozen and stored analysis in the environmental chemistry laboratory at SARDI Aquatic Sciences following standard methods (APHA-AWWA-WPCF 1998). Dissolved ammonium (NH_4^+, detection limit 0.071 µM), oxides of nitrogen (NO_x, detection limit 0.071 µM), phosphorus (PO_4^{3-}, detection limit 0.032 µM) and silica (SiO_2, detection limit 0.333 µM), were determined by flow injection analysis with a QuickChem 8500 Automated Ion Analyser. Results below the detection limit are assumed to be half the detection limit.

Following (Patten et al. 2018), 1 milliliter samples for bacteria were fixed in glutaraldehyde (0.5% final concentration), placed in the dark for 15 minutes, then quick frozen in liquid nitrogen and stored at -80 °C until analysis. Samples of bacteria were thawed at 37 °C, diluted 10 fold in Tris EDTA (pH = 8.0, Sigma-Aldrich), stained with SYBR I green (0.5×10^{-4} final concentration, Molecular Probes) in the dark at 80°C for 10 minutes and then 1.0 µm fluorescent beads (Polysciences) were added as an internal standard. Bacteria were analysed on a FACSVerse (Becton Dickenson) flow cytometer with an acquisition runtime of 2 minutes. Bacteria were discriminated on the basis of green fluorescence, side-angle light scatter (SSC) and forward-angle light scatter (FSC) using FlowJo® flow cytometry analysis software. Bacteria were separated on

plots of side scatter (SSC) and green (SYBR) fluorescence and SSC and red chl *a* fluorescence. *Prochlorococcus* often coincided with the stained bacterial group. To correct for this, *Prochlorococcus* were included within the bacterial group. Bacteria counts were then corrected by subtracting total counts of *Prochlorococcus* (obtained from non-stained samples) from the stained bacterial group. One milliliter samples for pico- and nanophytoplankton were fixed with paraformaldehyde glutaraldehyde (0.25% final concentration), quick frozen in liquid nitrogen and stored at -80°C until analysis. Picophytoplantkon samples were thawed at 37°C and 1 μm beads (Polysciences) were added as an internal reference. Samples were analysed on the same flow cytometer as above, with an acquisition run for 3 to 5 minutes. Different pico- and nanophytoplanton groups were discriminated on the basis of red and orange autofluorescence of chlorophyll, the accessory pigment phycoerythrin, and light scatter properties of side-angle light scatter and forward-angle light scatter.

The concentration of chl a is a proxy for phytoplankton biomass and was measured by fluorometry. Two litre water samples were filtered through Whatman GF/F filters (nominal pore size 0.4 μm). Filters were snap-frozen and stored at -80°C prior to analysis. Samples were extracted in 100% acetone overnight at -20ºC. Fluorescence readings were obtained from a Synergy4 multiplate reader calibrated using Sigma chlorophyll *a* standards at excitation and emission wavelengths of 430nm and 663nm, respectively.

The pigment composition of water samples was measured using High Pressure Liquid Chromatography (HPLC). Two litre water samples were filtered through Whatman GF/F filters (nominal pore size 0.4 μm). Filters were snap-frozen and stored at -80°C prior to analysis via the gradient elution procedure of Van Heukelem and Thomas (2001) on an Algilent 1200 series HPLC system in the environmental chemistry laboratory at SARDI Aquatic Sciences.

The TSS content of water samples was evaluated by filtering 500 mL samples through pre-combusted Whatman GF/F filters (nominal pore size 0.4 μm). Filters were oven dried at 60°C for 48 hours followed by combustion in a muffle furnace at 500°C for 1 hour in the environmental chemistry laboratory at SARDI Aquatic Sciences.

A detailed inventory of phytoplankton taxa and their cell abundances was obtained from one litre samples fixed with acidified Lugol's iodine solution. Enumeration and identification of phytoplankton to genus or species level was carried out using traditional methods by Microalgal Services, Victoria, Australia.

Zooplankton net samples were rinsed through a 35 µm mesh sieve to remove all traces of formalin prior to enumeration. The contents of the sieve were then rinsed into 100 ml measuring cylinders and allowed to settle for 24 hours, after which settling volumes were recorded. Zooplankton were identified to the lowest possible taxonomic level via microscopy, using standard taxonomic methods. Organism numbers were reported as individuals/m^3, according to the volume swept by the net. Volume swept was calculated as the distance travelled by the net (estimated using a General Oceanics flow meter suspended in the mouth of the net) multiplied by the area of the net mouth. Settling volumes were recorded in ml m^{-3} using the volume swept, and were converted to displacement volumes using a factor for samples without gelatinous zooplankton (0.35) (Wiebe et al. 1975, Wiebe 1988). Displacement volumes were then converted to biomass (mg C) using a factor of 21 for samples with displacement volumes < 1 ml, and a factor of 41 for samples with displacement volumes 1-10 ml (Bode et al. 1998).

Statistical Analysis

The stoichiometric nutrient ratios required to support phytoplankton growth given by the Redfield ratio (Redfield 1963) (C:N:P = 106:16:1) were extended to include silica (N:Si = 1:1) and assessed following the criteria of Tanner and Volkman (2009). Potential nutrient limitation required both (i) low concentrations of dissolved inorganic nitrogen (DIN =NO_x + NH_4^+), silica <0.5 µm and phosphorus <0.05 µm; and (ii) variations of the nutrient ratios away from the Redfield ratio.

Analysis of phytoplankton pigment composition was undertaken to provide an additional means of assessing changes in the phytoplankton community composition as a function of chl a biomass (Paerl et al. 2003). Following Claustre (1994), the biomass ratio of new to total production, referred to as the F_p ratio, was determined from the ratio of multiple pigments present in the phytoplankton community, and provides a simple indicator of trophic status. F_p values range between 0 and 1, with increasing values indicating a shift from oligotrophic (~0-0.3) through mesotrophic (~0.3-0.6) to eutrophic (>~0.6) conditions.

For individual variables, Analysis of Variance (ANOVA) was used to detect differences between years, months (i.e. seasons) and sites. Student t-tests were used to detect pairwise differences between sites, months and years, as appropriate, with *P* values <0.05 considered statistically significant for all analyses. Measures of variability around mean values are reported as the standard error (se) unless otherwise stated.

To better understand carbon flow and the influence of environmental factors on variations in planktonic community structure, the carbon biomass for several key autotrophic and heterotrophic groups of the planktonic ecosystem was estimated based on published empirical relationships (Fukuda et al. 1998, Menden-Deuer and Lessard 2000, Marquis et al. 2011). Carbon conversion factors of 0.020, 0.034, 0.076 and 1.0 pg C per cell were applied to bacteria, *Prochlorococcus*, *Synechococcus* (picophytoplankton) and picoeukaryote (nanophytoplankton) (Fukuda et al. 1998) abundances determined by flow cytometry. Carbon conversions of 531 per cell were applied to dinoflagellate and 'other' flagellates abundances, and 249 pg C per cell to diatom abundances obtained from microscopy (Menden-Deuer and Lessard 2000, Marquis et al. 2011). Zooplankton biomass was estimated from settling and displacement volumes as described in the Appendix.

Statistical analyses of phytoplankton abundance data for key functional groups (diatoms, dinoflagellates and 'other' flagellates, in units of cells/L) and plankton community carbon biomass data (in units of µg C/L) was carried out to examine differences between years, months and sites using PERMANOVA and non-metric multidimensional scaling (nMDS) with the Primer 7.0.11 software package (Clarke and Gorley 2015), and the PERMANOVA+ add-on (Anderson et al. 2008). Phytoplankton abundance data and planktonic carbon biomass data were fourth root transformed to downweight the influence of abundant groups, and resemblance matrices were calculated using the Bray-Curtis index to eliminate the influence of joint absences of groups. 9999 permutations were undertaken under a reduced model to calculate significance levels. Pair-wise comparisons were run to test the significance of differences between sites, months and years, with *P* values <0.05 considered statistically significant for all analyses.

The influence of environmental factors on variation in planktonic community structure was examined using a distance based linear model (DistLM) and distance based redundancy analysis (dbRDA). Environmental data (temperature, dissolved nutrients) were $\log_{(x+1)}$ transformed and normalised prior to running DistLM and dbRDA, with the Akaike information criterion (AIC) used for best model selection.

Coupled Hydrodynamic-Biogeochemical Model

The hydrodynamic model is based on the Regional Ocean Modeling System (ROMS), and corresponds to a reduced-resolution version of the Two Gulfs Model (TGM), available through eSA-Marine (https://pir.sa.gov.au/research/esa_marine) coupled to the Fennel et al. (2006)

biogeochemical model (Middleton et al. 2013). The model includes both gulfs, with open boundaries prescribed by the Bluelink Reanalysis (BRAN, Oke et al. 2013) so as to allow the exchange of dense salty, cold water during autumn to winter. Surface atmospheric forcing is provided by NCEP Climate Forecast System Reanalysis Version 2 (Saha et al. 2014), and tidal forcing provided by TPXO8 (Erofeeva and Egbert 2014). Chlorophyll a and dissolved inorganic nitrogen boundary conditions are provided from the South Australian Integrated Marine Observing System (IMOS, http://imos.org.au/). Anthropogenic nitrogen loads were estimated from monthly feed data reported to PIRSA F&A following Fernandes et al. (2007) and Fernandes and Tanner (2008), and are input into the model as NH_4^+. Annual wastewater treatment plant (WWTP), including the Port Lincoln WWTP, and Onesteel nitrogen loads were downloaded from the National Pollution Inventory (http://www.npi.gov.au/) and are input into the model as both NO_x and NH_4^+, consistent with previous modelling studies for Spencer Gulf (Middleton et al. 2013, Doubell et al. 2015). The model resolution is 1500m in the horizontal, with 15 sigma levels in the vertical, and is run with a 200 second time step. Model output is stored at the AEMP sampling sites at half hour intervals, with daily values stored at all grid points. Three-day averages are also saved at all grid points for updating the CarCap software.

2.3. Results and Discussion

Physical Environment: Regional Oceanography and hydrodynamic model validation

The location of the mooring site (LRS) is shown in relation to the topography of the region of study in Figure 2.1. Hourly observations of (depth-averaged) currents, temperature and salinity were obtained for the period January to May in 2017 and 2018. In 2016 current data was only collected for January and February due to failure of the ADCP current profiler in March. In order to understand the hydrodynamics of the region and validate the hydrodynamic model, mooring observations are compared to model predictions and are evaluated with respect to the dominant forcing mechanisms (e.g. tides, weather events).

Tidal Currents

The time series of observed and model tidal currents for 2016, 2017 and 2018 have been resolved along the principal axis (i.e. major current direction) of the tides, which is directed to the north (Figure 2.2). Tidal currents along the principal axis reach up to ~0.4 m/s. Minor axis components are much smaller, with variability of 0.1 m/s or less. The agreement between model and observed principal axis currents is excellent, with r^2 greater than 0.91: r^2 is a measure of the fraction of variability (variance) of the data that is explained by the model. The root mean square error (RMSE) is < 0.05 m/s (approximately 1/10th of the tidal signal). The bias is the difference between the mean of the observed and model time series, and is negligible. The tidal signals also fall to near zero every 14 days (the "dodge" tide), as expected for a tidal signal that is dominated by the M_2 and S_2 semi-diurnal tides.

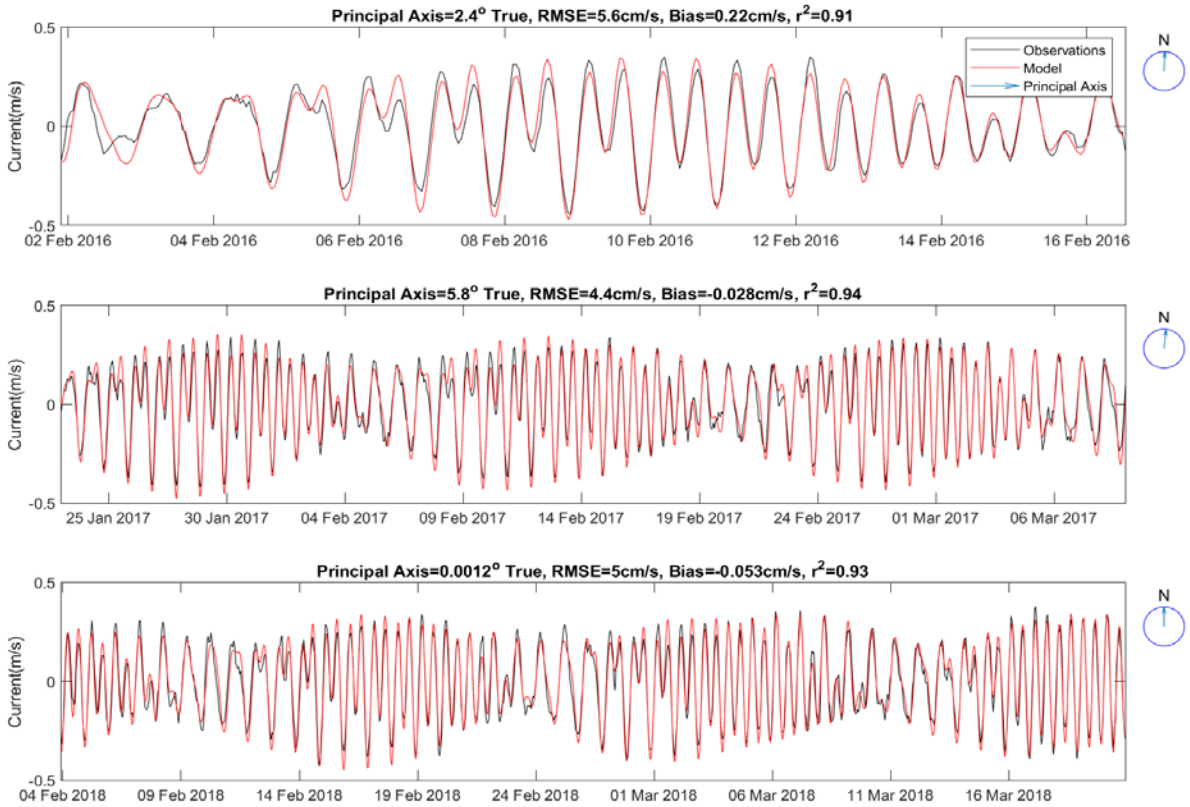

Figure 2.2: Time series of observed (black line) and model (red line) tidal currents using vertically averaged model and ADCP currents (m/s) resolved along the principal axis of the observations for each of the mooring deployment periods at the site LRS. The direction of the principal axis is illustrated in the blue compass to the right of each time series. Directions are positive to the north. Only the first 6 weeks of 2017 and 2018 observations are plotted to better resolve the comparisons. The top, middle and bottom panels present results for 2016, 2017 and 2018, respectively.

Low frequency currents – tidal residuals

Currents driven by weather band events over periods of 3-10 days were resolved along the principal axis by applying the Thompson (1983) tide-filter to remove the tidal signal (Figure 2.3). The model and observations both show current variability at periods of 3 to 10 days, with amplitudes up to ~0.1 m/s. These currents are weaker than those generated by tides and agreement between model and observed principal axis currents is reasonable to good with r^2 values of 0.39 and 0.56 for 2017 and 2018. Importantly, the model generally reproduces the observed weaker circulation, including some weather-band events. The origin of these 3 to 10 day motions is likely due in part to wind stress (Figure 2.3), as indicated through the clear correspondence between many of the ocean current and wind stress events.

Figure 2.3: Time series of observed (black line) and model (red line) residual currents using vertically averaged model and ADCP weather-band currents (tidal residuals) (m/s) at the mooring site LRS resolved along the principal axis of the observations for each of the mooring deployment periods. The direction of the principal axis is illustrated in a compass to the right of each time series. Positive currents are to the NNE for 2017 and 2018. Comparison statistics are shown above each plot. In addition, the magnitude of the low pass filtered wind stress from the mooring site LRS is also presented in each plot (green curves) and the vertical lines illustrate several wind forced events in the low pass filtered currents.

Plan views of the monthly averaged model currents for the study region were used to interpret the regional circulation at longer time-scales (Figure 2.4). The modeled circulation shows considerable inter-annual variation in January. The very weak model currents (<0.02 cm/s) vary in direction at the mooring site. For May, the monthly average currents are stronger than for January, and directed predominantly to the north. These results are consistent with the expected blocking of the gulf during summer and the large, gulf-scale clockwise circulation expected for autumn/winter; when cold salty water flows out along the eastern side of Spencer Gulf and shelf water flows in along the western side the gulf.

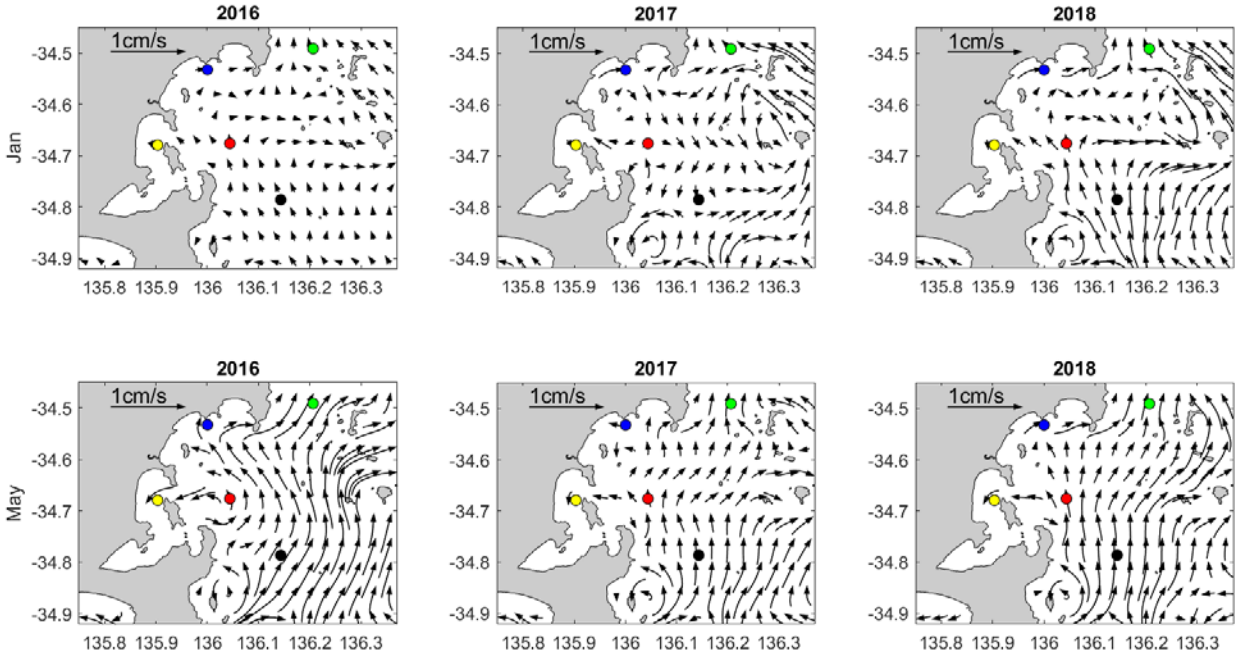

Figure 2.4: Monthly averages of the model vertically averaged currents (cm/s) for the survey region 2016-2018. The top row shows the January averages and the bottom row shows the May averages for each of the 3 years of study. A vector length of 1 cm/s is shown. Sampling sites are illustrated with colored markers and the mooring site (LRS) indicated by the black circle.

Monthly averaged observed and model currents at the LRS mooring site differed by month (Figure 2.5). In 2017, the observed monthly averaged flow is to the north (0.03 m/s), but it is near zero during 2018. Model results indicate that flow at the mooring site is to the south during summer, particularly during 2018, and then to the north or north-east after approximately 26th March. This outcome is consistent with the expected summer blocking of the gulf and clockwise circulation noted above: there is some difference as to timing. We have no explanation for the observed summer northward flow except that the monthly mean (model) currents (Figure 2.4) are weak and display considerable inter-annual and spatial variability. Both the model and observations for May show a stronger northward flow that is consistent with the expected inflow along the western side

of the gulf and the gulf-scale clockwise circulation expected for the region (Nunes and Lennon 1987, Nunes Vaz et al. 1990).

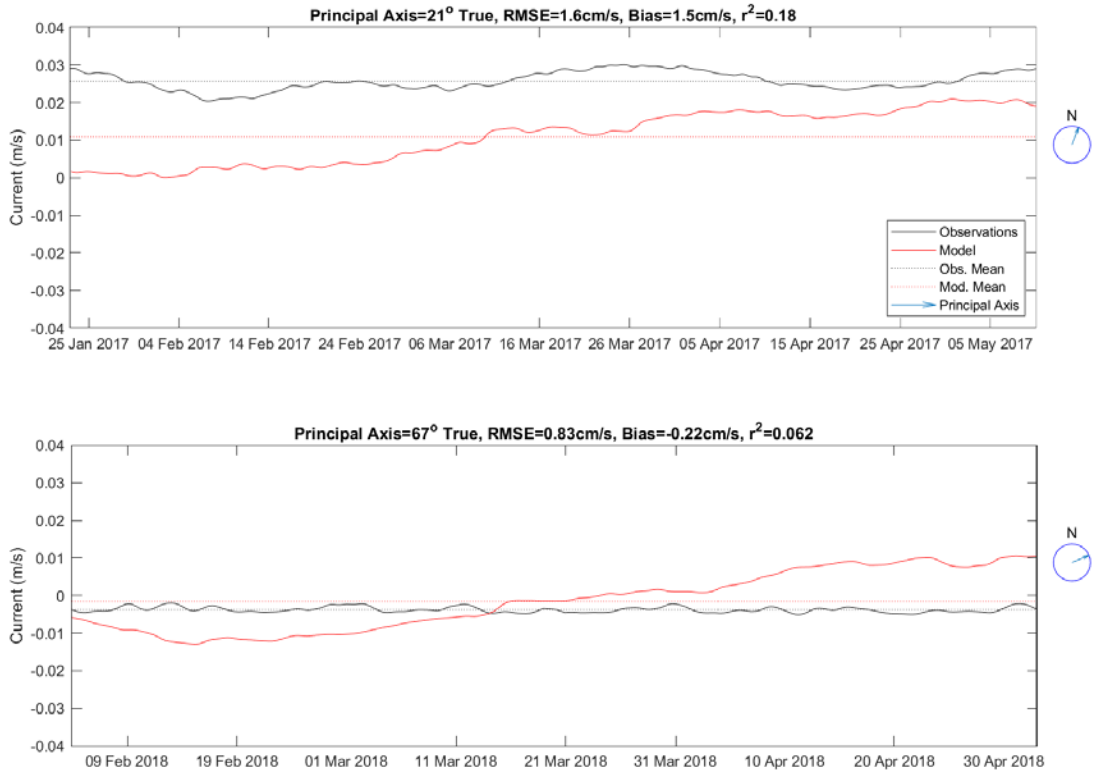

Figure 2.5: Comparison of vertically averaged model and ADCP 30-day moving-average currents (m/s) at site LRS resolved along the principal axis of the observations for each of the mooring deployment periods. The direction of the principal axis is illustrated in a blue compass to the right of each time series. Comparison statistics are shown above each plot.

Temperature

The accurate prediction of temperature (and salinity) by the ocean model is important for modelling the density driven circulation within Spencer Gulf, and both strongly influence the physiological processes of plankton and other organisms (e.g. finfish). Time series plots of observed and model temperature were obtained at a depth of 20 m from the moored CTD and are presented in Figure 2.6. The first notable feature is the 12 hour tidal variations, with changes

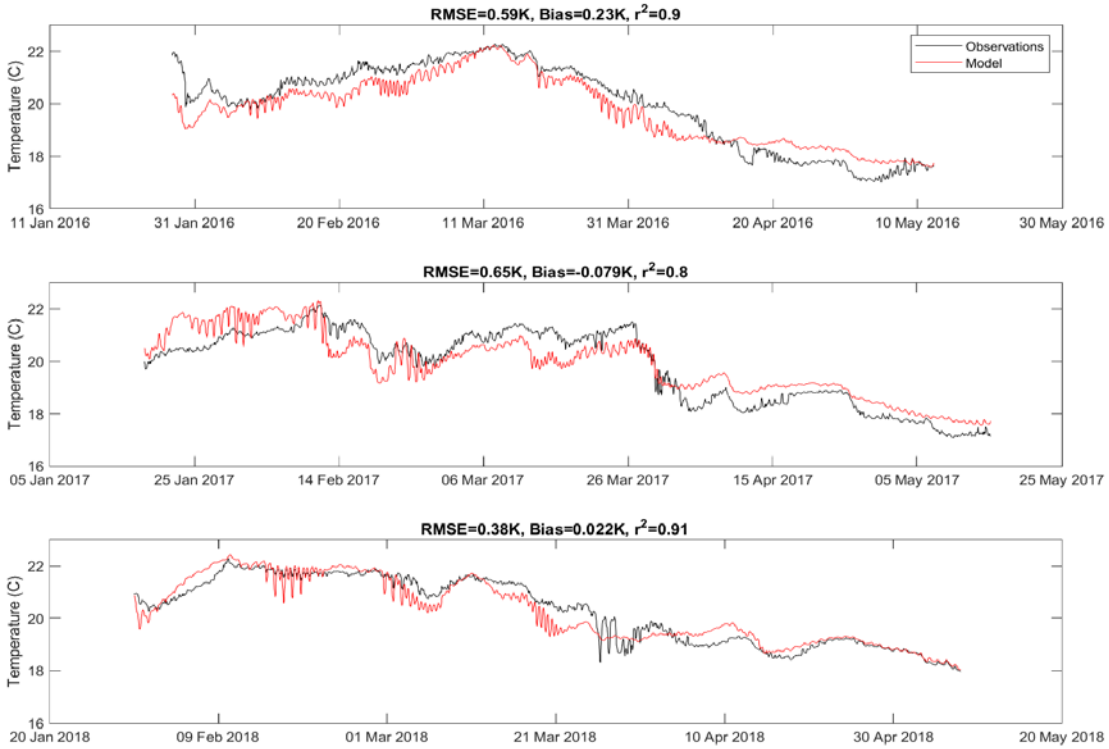

Figure 2.6: Comparison of the 20 m depth model and CTD temperature (°C) at site LRS for each of the mooring deployment periods. Comparison statistics are shown above each plot.

in temperature (dT) of up to 1°C. In general, the magnitude of these variations is captured by the model, and they result from tidal advection of the temperature field, which must therefore have some spatial variation across the region. To estimate this spatial variation in temperature, consider the following model for tidal displacement. The maximum tidal speed v_0 from Figure 2.2 is about 0.4 m/s so that the semi-diurnal velocity in the north/south direction may be written as;

$$v = v_0 \sin(\omega t) \quad (1)$$

where $\omega = 2\pi/T$ is the semi-diurnal frequency, T = 12 hours (the tidal period) and t is time. Integrating v(t) with respect to time yields the tidal displacement

$$Y(t) = (T v_0)/ 2\pi \cos(\omega t) \quad (2)$$

that implies a maximum (peak to peak) displacement of

$$Y_{max} = (T v_0)/ \pi \sim 5 \text{ km} \quad (3)$$

The maximum north/south temperature gradient dT/dy associated with the tidal displacement (3) is then

$$dT/dy = dT/Y_{max} = 1.0/ (5000)\ ^oC /m \quad (4)$$

or 1^{o}C per 5 km.

Using the above methodology and estimated temperature gradient (eqn 4), the temperature variation due to the weather-band model variability may also be estimated. Assuming a weather-band period of P= 3 days, and a velocity of $v_0 = 0.07$ m/s (Figure 2.3), a peak to peak displacement of $Y_{max} = 8$ km is obtained. The associated peak to peak temperature variability is then obtained from,

$$dT=(dT/dy)* Y_{max} = (1.0/5000)*8000 = 1.6\ ^oC \quad (5)$$

where dT/dy is given by (eqn 4). The value (eqn 5) is perhaps twice that evident from the weather-band variability evident in Figure 2.7, where the time series have been low pass filtered, suggesting that the assumptions made above are at best approximate. This comparison shows that while the magnitude of the tidal and weather-band temperature variations is reproduced by the model, specific details (i.e. events) are not always reproduced. Local heating has been identified to account for up to 50% of temperature variations for the region (Hertzfeld et al. 2009) and may therefore be important.

We note the tidal and weather-band temperature variations discussed above are relatively small compared to the 4^{o}C change observed between February and May. All three years of data (Figure 2.7) show the presence of cooler water during March, which is again consistent with the breakdown of the summertime blocking and the northward advection in autumn due to the presence of a large-scale clockwise circulation within Spencer Gulf. Comparison of the observed low-pass filtered observations with model output showed $r^2>0.79$, indicating the model reproduces the observations, and therefore the timing of autumn inflow of shelf water into the gulf quite well.

CTD profiles show the water is well mixed in the vertical at almost all sites (Figure 2.8). Warmer (colder) water is found at the nearshore sites BXZ and BRN during January (May). This is likely the result of local summer heating or autumn/winter cooling in the shallower coastal waters. May temperatures are generally about 3 to 4^{o}C cooler than summer temperatures. For the 3 offshore sites (LRS, LFZ, LRN), the spatial gradients dT/dy may be determined as about 1^o C per 30 km

for summer. This less than that estimated from the mooring data (1° C per 5 km), indicating estimates using the simple tidal model (eqn 4) are at best order of magnitude accurate.

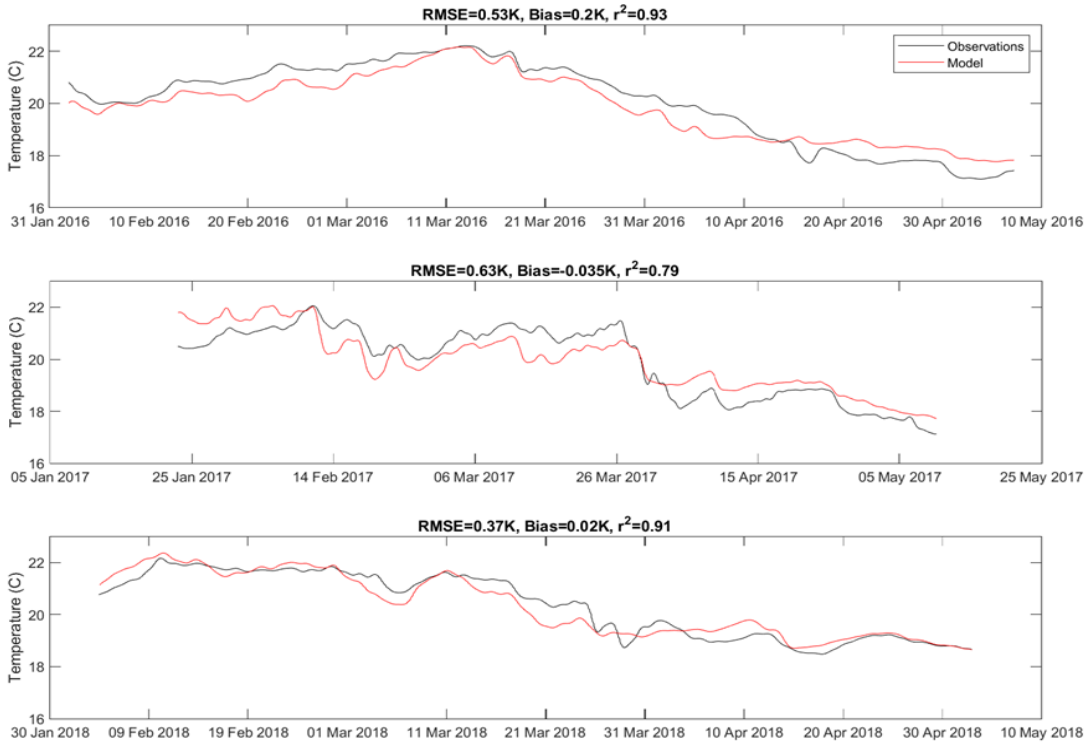

Figure 2.7: Comparison of the 20 m depth model and CTD temperature (°C) at site LRS for each of the mooring deployment periods. Temperatures have been filtered to remove variations associated with tidal currents. Comparison statistics are shown above each plot.

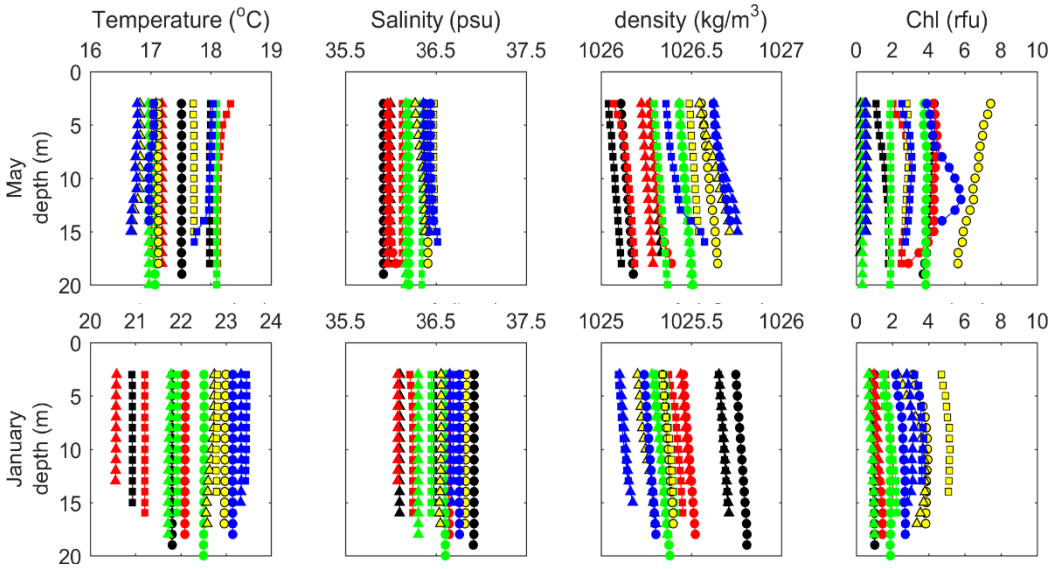

Figure 2.8: CTD profiles (and chlorophyll a fluorescence) as sampled in May (upper panels) and January (lower panels) for the years 2016 (circles), 2017 (triangles), and 2018 (squares) and at each of the color coded sites as shown in Figure 2.1.

Salinity

There is very weak salinity variability due to tidal advection (not shown). As for temperature, there is a marked freshening of water each year during and following March (Figure 2.9). This is consistent with the expected gulf-scale clockwise circulation and an inflow of cold, fresh seawater on the western side of Spencer Gulf. This freshening is opposite to the increase in salinity expected from local evaporation, which by itself will act to increase salinity all year round. The observed decrease of 1 psu (Figure 2.9) strongly suggests that the freshening arises from advection by the gulf-scale clockwise circulation. Salinity estimates were also obtained from the January and May CTD profiles for each site (Figure 2.8). The saltiest sites during January and May are generally those closest to the coast. Like heating, local evaporation will be more effective in shallower coastal waters.

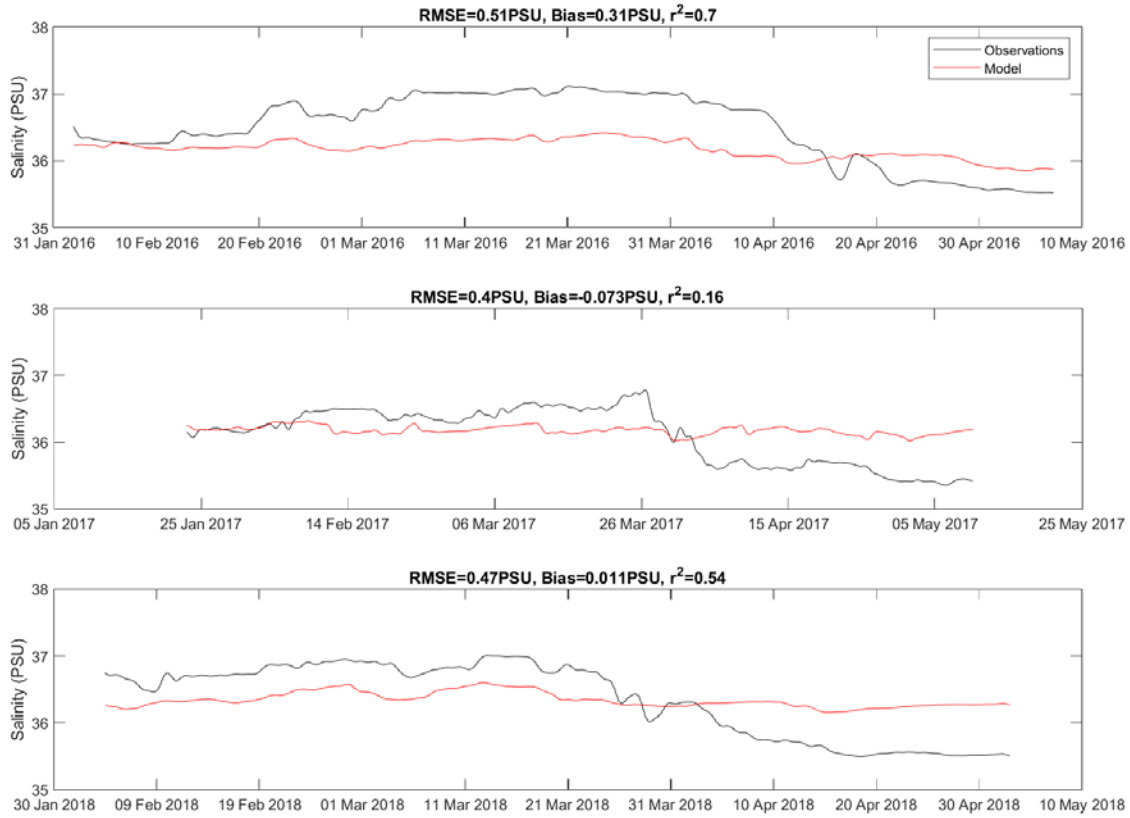

Figure 2.9: Comparison of the 20 m model depth and CTD salinity (PSU) at site LRS for each of the mooring deployment periods. Salinities have been filtered to remove variations associated with tidal currents. Comparison statistics are shown above each plot.

Anthropogenic Inputs

Quantifiable sources of anthropogenic nutrients into Spencer Gulf include those from finfish aquaculture, waste water treatment plants (WWTP) and the OneSteel steelworks, all of which are included as inputs into the biogeochemical model.

Anthropogenic nutrients loads into the Port Lincoln region were dominated by aquaculture. Annual total dissolved inorganic nitrogen load estimates from SBT and YTK aquaculture increased from 1536 t in 2016 to 1548 t in 2017 and 1721 t in 2018. Baitfish accounted for approximately 83% of the total annual nitrogen load. Manufactured feed and the Port Lincoln WWTP contributed 16 % and less than 1% of the annual nitrogen inputs into the region, respectively. Monthly loads generally peaked during April or May, with a maximum of 380 tons occurring in April 2018 (Figure 2.10). These loads are approximately 10 % less than the annual (1946 t) and peak monthly loads (409 t) previously reported for 2006 (Tanner and Volkman 2009).

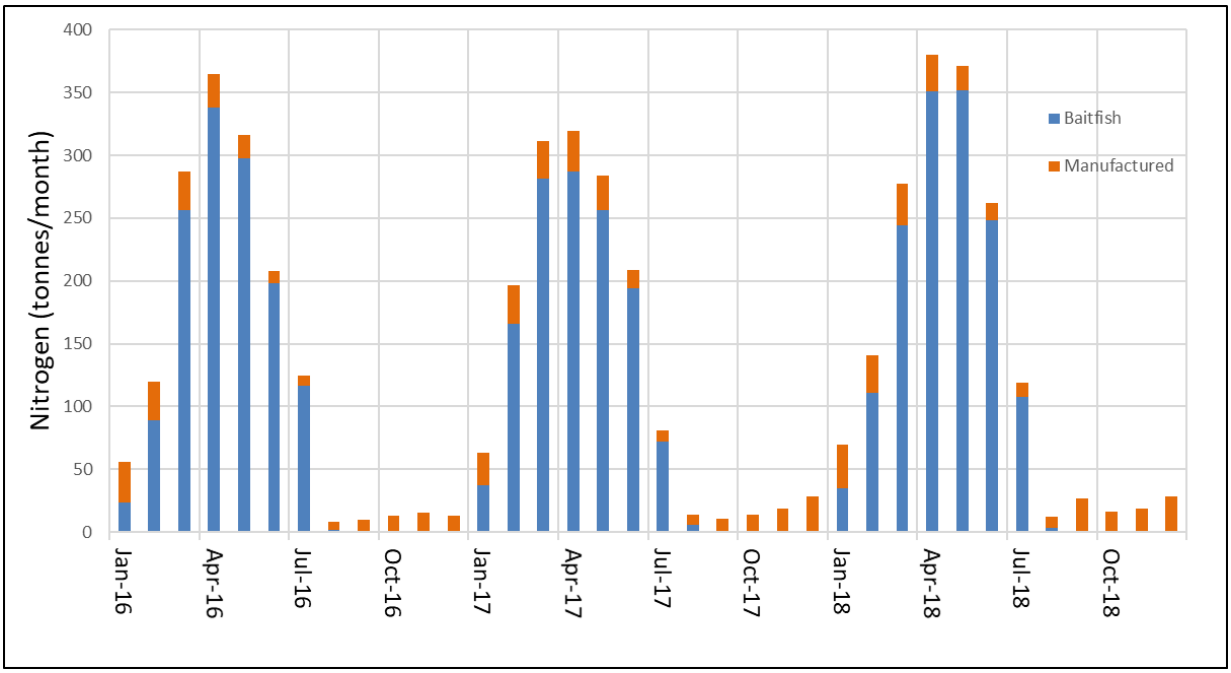

Figure 2.10: Estimated monthly loads of dissolved inorganic nitrogen (tonnes/ month) from aquaculture. Blue and orange colors indicate the nitrogen component for the two main feed types; baitfish and manufactured.

Biogeochemical Model

Modelled and observed NO_x, NH_4^+ and chl a concentrations were in reasonable to good agreement (Figures 2.11 and 2.12) and below the ANZECC/ARMCANZ (2000) water quality

guideline concentrations of 3.6 µM (~ 50 µg/L) for NO_x and NH_4^+ and, with the exception of January 2016 (Figure 2.12, Table 2.2), typically around or below the 1 µg/L guideline concentration for chl a. NO_x concentrations at LRS were in good agreement, indicating the model reproduces the NO_x flux from the shelf into the gulf. The model slightly over-predicts NO_x concentrations at other sites (Figure 2.11). Model sensitivity studies indicate this may be due to either an underestimate of the microbial remineralization rates or the portioning of NO_x from anthropogenic sources (e.g. aquaculture feed inputs are input as only NH_4^+). The model provides good predictions for NH_4^+ concentrations. Chl a concentrations are also generally well predicted by the model, with the exception of a few high concentrations observed during January 2016 (see Figure 2.16).

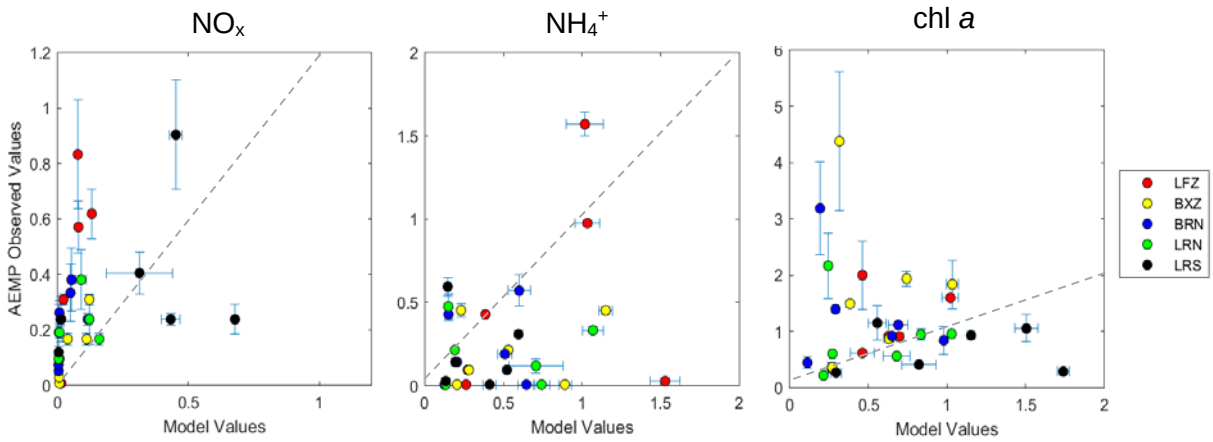

Figure 2.11: Comparison of observed concentrations versus corresponding daily averaged model values for oxides of nitrogen (NO_x), ammonium (NH_4^+) and chlorophyll a (chl a). The ANZECC/ARMCANZ (2000) water quality guideline concentrations are 3.6 µM for NO_x and NH_4^+ and 1 µg/L for chl a.

Time series of modelled predictions at four representative sites provide insights into circulation and nutrient supply dynamics in the region (Figure 2.12). In agreement with the observations, NO_x, NH_4^+ and chl a concentrations are typically low, with small autumn signatures observed for NO_x and chl a at LRS and little to no seasonal signature for NH_4^+. Compared to LRS, the seasonal signal at LFZ (and other sites) for NO_x is less in autumn, indicating phytoplankton uptake of NO_x supplied from the shelf has occurred. In contrast, NH_4^+ concentrations at LFZ are at their maximum in autumn, are correlated with aquaculture inputs (see Figure 2.10), and at times approach the ANZECC/ARMCANZ (2000) water quality guideline concentrations (3.6 µM). During autumn there is a corresponding peak in chl a concentrations at LFZ. NH_4^+ concentrations at inshore sites (BXZ and BRN) follow those observed at LFZ, but at reduced concentrations due to both dilution and phytoplankton uptake. The model slightly under-predicts the observed chl a

concentrations at BXZ and BRN, possibly due to the corresponding slight under-prediction of NO_x levels for the reasons discussed. Model simulations for 2016, 2017 and 2018 using the coupled hydrodynamic-biogeochemical model have been included in an update of the 'CarCap' software (Figure 2.13) and provided to PIRSA F&A to assist in regional aquaculture management and planning.

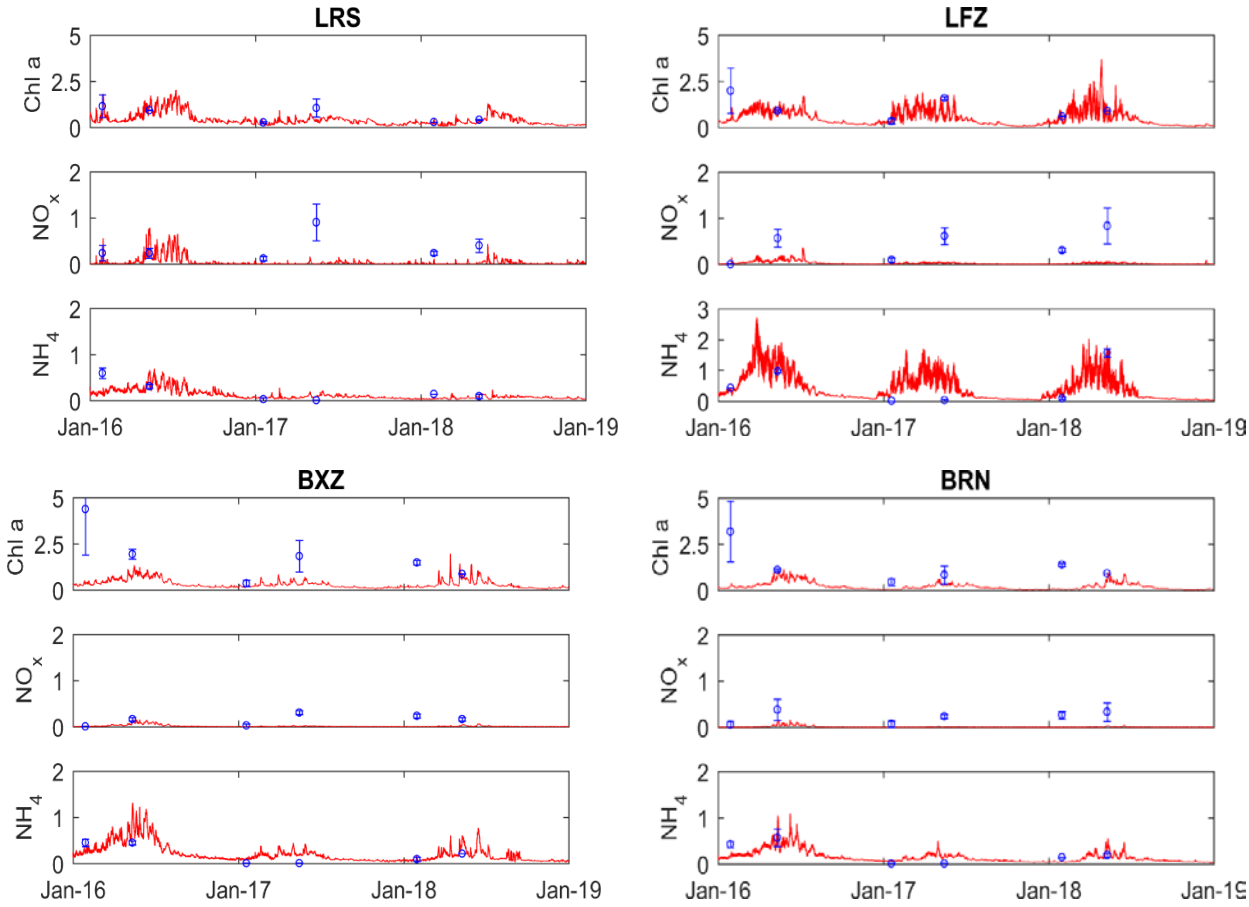

Figure 2.12: Modelled depth-averaged time-series of chlorophyll a (chl a, µg/L), nitrate (as NO_x, µM) and ammonium (NH_4^+, µM). Field measurements are overlaid for comparison (blue markers, mean ± standard deviation). Note change in vertical scale for NH_4^+at LFZ. The ANZECC/ARMCANZ (2000) water quality guideline concentrations are 3.6 µM for NO_x and NH_4^+ and 1 µg/L for chl a.

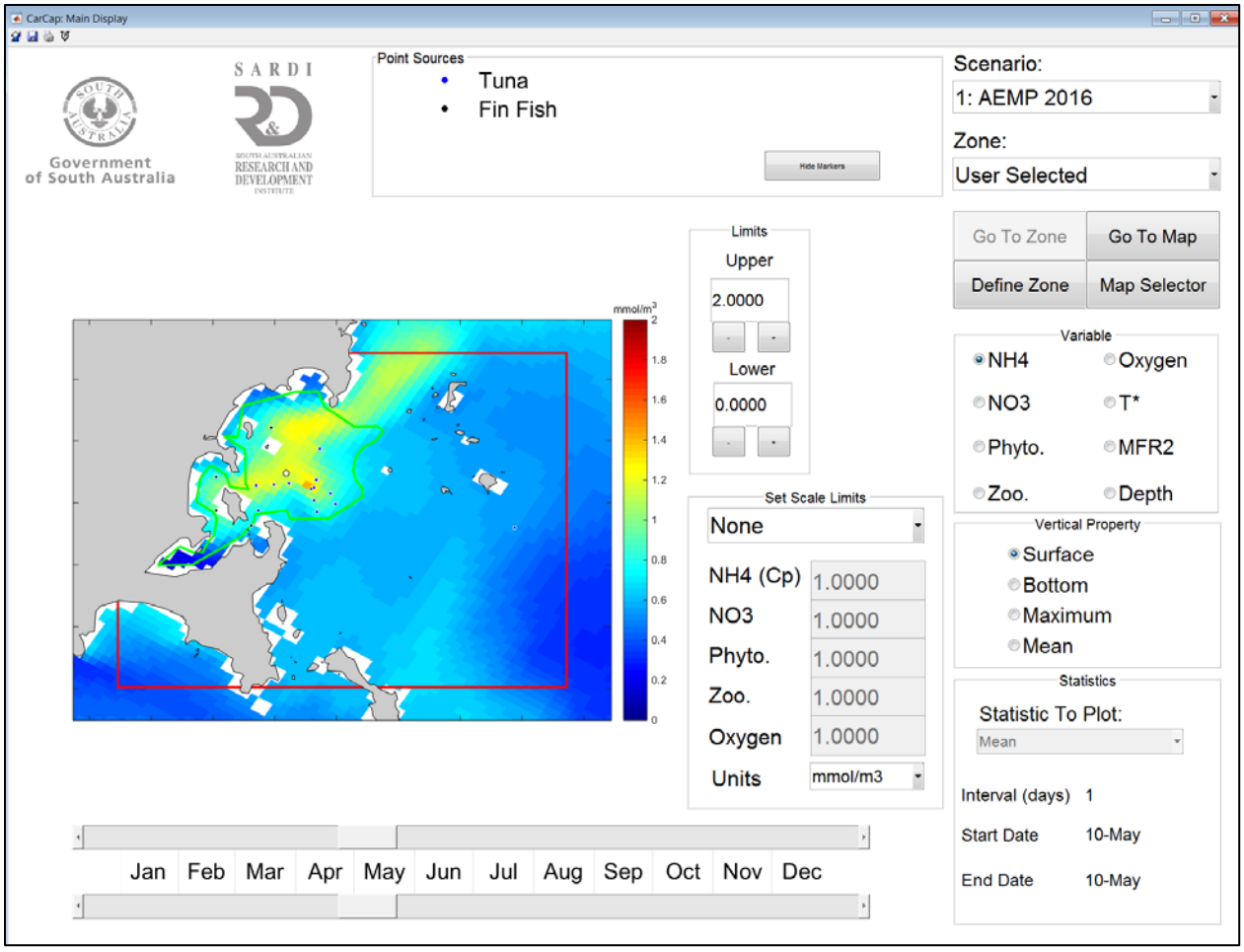

Figure 2.13: Screenshot of the CarCap model interface showing a snapshot of the modelled distribution of NH_4^+in the Port Lincoln region on May 10, 2016.

Water Quality: Nutrients, Chlorophyll-a and Turbidity

Mean nutrient concentrations for each site varied over the three surveyed years determined from triplicate samples (Figure 2.14). NO_x concentrations were generally low and ranged from the detection limit to a maximum 0.904 ± 0.131 µM at LRS in May 2017. Table 2.1 shows there were significant differences in NO_x concentrations between months, with January concentrations averaged across all sites and years (0.143 ± 0.003 µM) lower than May concentrations (0.397 ± 0.006 µM; Table 2.2). Whilst not significant, May concentrations at offshores sites decreased along a gradient from LRS to LFZ and LRN and were greater than those observed inshore at BXZ and BRN (Figure 2.14), consistent with the biogeochemical model results (Figure 2.12).

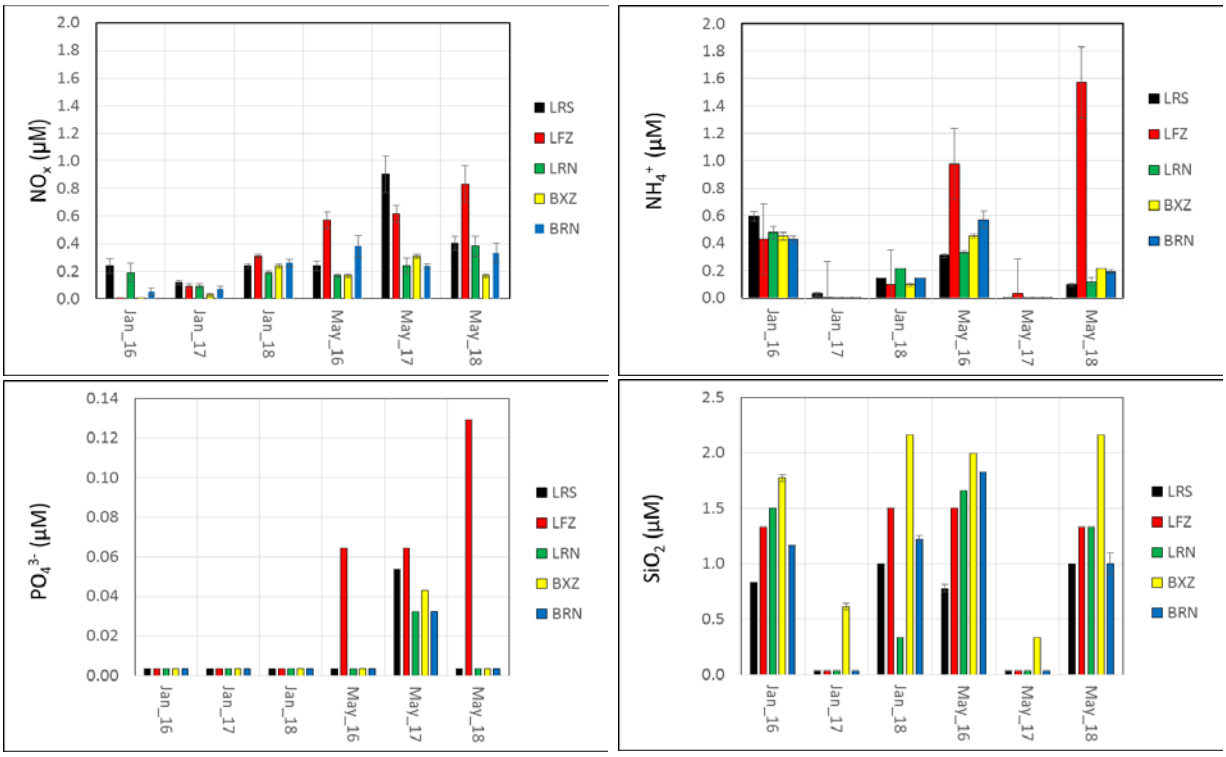

Figure 2.14: Mean nutrient concentrations for each site measured in January and May 2016, 2017 and 2018. Error bars are ± 1 standard error.

Table 2.1: ANOVA results for NO_x concentrations by year, month and site.

Source	df	SS	F	P
Year	2	0.085	1.234	0.341
Month	1	0.604	17.434	**0.003**
Site	4	0.262	1.892	0.205
Year x Month	2	0.171	2.470	0.146
Year x Site	8	0.304	1.097	0.450
Month x Site	4	0.152	1.095	0.421
Residual	29	1.854		

Table 2.2: Mean nutrient, chlorophyll a and total suspended solid (TSS) concentrations averaged across all sites for each January and May and survey year. Mean seasonal concentrations and standard errors (se) averaged across all survey years are given in bold type. The ANZECC/ARMCANZ (2000) water quality guideline concentrations are 3.6 µM for NO_x and NH_4^+ and 1 µg/L for chl a.

Month	Year	NO_x (µM)	NH_4^+ (µM)	$P0_4^{3-}$ (µM)	SiO_2 (µM)	Chl *a* (µg/L)	TSS (mg/L)
January	2016	0.099	0.476	0.003	1.320	3.278	16.888
	2017	0.082	0.011	0.003	0.149	0.330	4.640
	2018	0.247	0.138	0.003	1.243	0.878	6.284
	mean	**0.143**	**0.208**	**0.003**	**0.904**	**1.495**	**9.271**
	se	**0.003**	**0.005**	**0.000**	**0.015**	**0.035**	**0.378**
May	2016	0.305	0.528	0.015	1.553	1.169	3.759
	2017	0.462	0.011	0.045	0.093	1.257	16.304
	2018	0.424	0.438	0.028	1.365	0.734	3.749
	mean	**0.397**	**0.326**	**0.030**	**1.004**	**1.053**	**7.937**
	se	**0.006**	**0.010**	**0.001**	**0.017**	**0.011**	**0.359**

NH_4^+ concentrations ranged from the detection limit up to 1.57 ± 0.048 µM at LFZ in May 2018, with the highest concentrations typically observed at LFZ in May. Table 2.3 shows there were significant differences in NH_4^+ concentrations between years. Pairwise comparisons showed mean concentrations averaged across all sites were significantly less in 2017 compared to 2016 and 2018 (Figure 2.14). Although not significant, NH_4^+ concentrations at LFZ in May were greater than observed at other sites (Figure 2.14), which is consistent with the biogeochemical model results (Figure 2.12).

Table 2.3: ANOVA results for NH_4^+ concentrations by year, month and site.

Source	df	SS	F	P
Year	2	1.182	12.576	**0.003**
Month	1	0.105	2.242	0.173
Site	4	0.451	2.400	0.136
Year x Month	2	0.079	0.836	0.468
Year x Site	8	0.286	0.762	0.645
Month x Site	4	0.584	3.107	0.081
Residual	29	3.063		

PO_4^{3-} concentrations were generally below the detection limit, particularly during January. There were significant differences in PO_4^{3-} concentrations between month, site and month and site (Table 2.4). Month was the most influential explanatory variable with elevated concentrations observed at LFZ in May 2016, 2017 and 2018 relative to other sites (Figure 2.14). The significant interaction between month and site suggests the effect of month is different between sites, which is likely due to the increased concentrations observed in May at LFZ.

Table 2.4: ANOVA results for PO_4^{3-} concentrations by year, month and site.

Source	df	SS	F	P
Year	2	0.001	1.864	0.216
Month	1	0.005	17.674	**0.003**
Site	4	0.006	5.121	**0.024**
Year x Month	2	0.001	1.864	0.216
Year x Site	8	0.002	1.000	0.500
Month x Site	4	0.006	5.121	**0.024**
Residual	29	0.024		

SiO_2 concentrations ranged from the detection limit up to 2.164 µM at BXZ in January 2018. There were significant differences in SiO_2 concentrations between year and site (Table 2.5). Year was the most influential explanatory variable, with concentrations averaged across all sites significantly less in 2017 compared to 2016 and 2018 (Figure 2.14). Spatially, pairwise comparisons showed concentrations at BXZ were significantly greater than those measured at LRS, with all other pairs of sites being similar.

Table 2.5: ANOVA results for SiO_2 concentrations by year, month and site.

Source	df	SS	F	P
Year	2	10.988	98.761	**< 0.001**
Month	1	0.092	1.660	0.234
Site	4	2.556	11.486	**0.002**
Year x Month	2	0.090	0.813	0.477
Year x Site	8	1.047	2.352	0.124
Month x Site	4	0.175	0.788	0.564
Residual	29	15.394		

Overall nutrient concentrations were generally low, with observed NO_x and NH_4^+ concentrations below the ANZECC/ARMCANZ (2000) guideline limits of 3.6 µM (~ 50 µg/L). With the exception of NO_x and PO_4^{3-}, the seasonal nutrient differences were weak and observed values were similar to previous measurements made in the tuna farming zone (Tanner and Volkman 2009). We note Tanner and Volkman (2009) reported no significant spatial variation in nutrients across the region. In contrast, we observed between site differences in the concentrations of NH_4^+ and PO_4^{3-} and SiO_2. This finding is consistent with NH_4^+ and PO_4^{3-} nutrients being supplied from local anthropogenic sources, including aquaculture feed (Fernandes et al. 2007), rather than via natural shelf/gulf exchange processes, and is supported by the model results for NH_4^+ (Figure 2.12). The source of SiO_2 responsible for the elevated concentrations observed at BXZ is unknown.

Examination of the nutrient ratios required to support phytoplankton growth following Redfield (1963) indicated that phosphorus, and to a lesser extent DIN, limitation was likely at all sites and

at different times, with the exception of LFZ in May (Figure 2.15). N:Si ratios indicate that nitrogen, and to a lesser extent silica, may also limit phytoplankton growth at times.

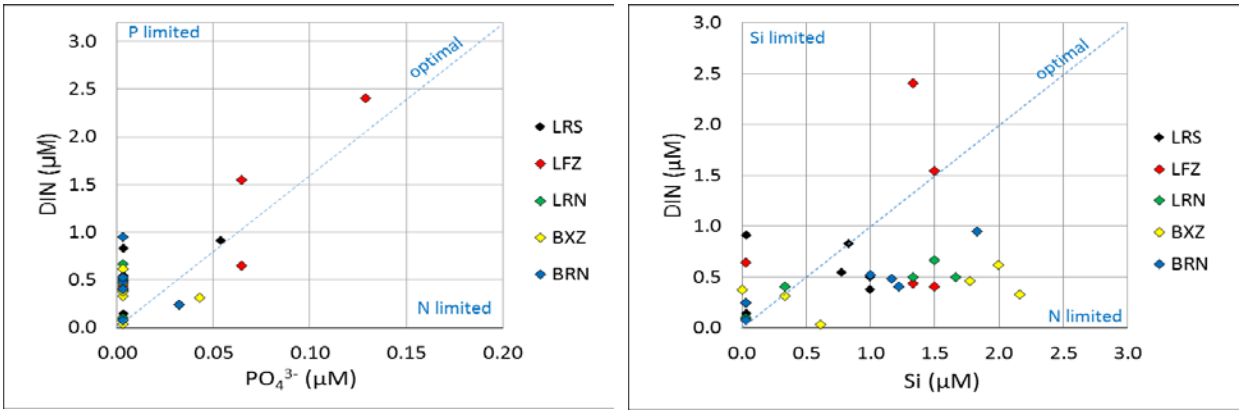

Figure 2.15: Nutrients ratios across for all sites and surveys for (left) dissolved inorganic nitrogen versus phosphate (right) dissolved inorganic nitrogen versus silicate.

Nitrogen is typically regarded as the nutrient limiting phytoplankton growth in marine systems (Howarth and Marino 2006), The results shown in Figure 2.15 are consistent with previous analysis of nutrient ratios and concentrations in the Lincoln and Boston Bay aquaculture farming region (Tanner and Volkman 2009, Middleton et al. 2013), and suggest nutrient availability is likely to limit phytoplankton growth in the region at times.

With the exception of January 2016, monthly mean chl a concentrations (Table 2.2) were generally around or below the ANZECC/ARMCANZ (2000) guideline limits of 1 µg/L and are consistent with previous measures reported for the region (Tanner and Volkman 2009, Middleton et al. 2013). There were significant differences in chl a concentrations between years, as well as a year by month interaction (Table 2.6). The significant interaction between year and month suggests the effect of year is different between months, which is likely due to the increased concentrations observed across all sites in January 2016 (Figure 2.16). In January 2016, chl a concentrations ranged between 1.460 ± 0.012 µg/L at LRS to 5.610 ± 0.064 µg/L at BXZ. The 3-year mean January concentration (1.495 ± 0.035 µg/L, Table 2.2) is about a factor of 2 higher than January concentrations previously reported for the region (Tanner and Volkman 2009, Middleton et al. 2013). Spatially, whilst not significant, concentrations were generally higher at the inshore sites (BXZ and BRN) and decreased offshore and with distance from LFZ; the lowest concentrations were observed at LRS. Concentrations greater than the ANZECC/ARMCANZ (2000) guideline limit of 1 µg/L were at times observed at LFZ, BRN and BXZ.

We note January 2016 chl a concentrations coincided with lower NO_x concentrations at many sites (Figure 2.14), suggesting NO_x availability/uptake may have been responsible for the elevated chl *a* concentrations observed at this time. However, overall there was a poor correlation between dissolved inorganic nitrogen (DIN = NO_x + NH_4^+) and chl a over the entire dataset (r^2 = 0.07).

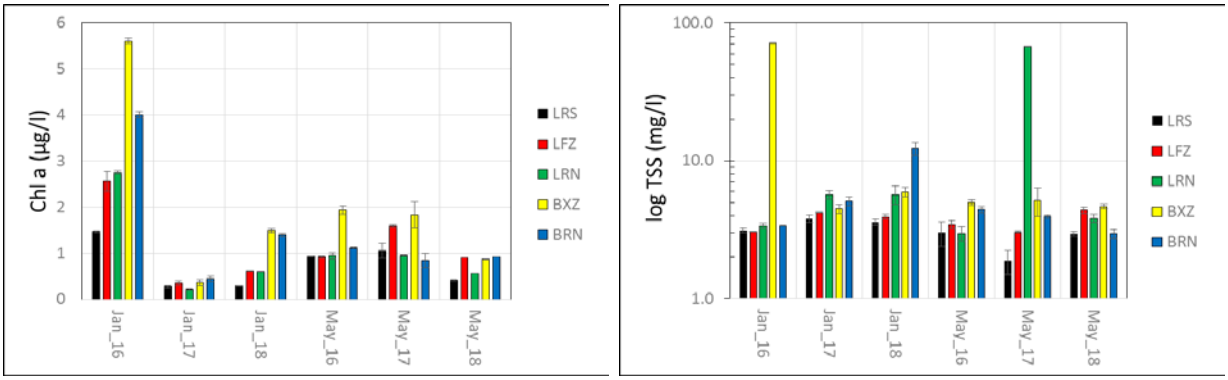

Figure 2.16: Mean chlorophyll a and total suspended solid (TSS) concentrations for each site measured in January and May 2016, 2017 and 2018. Error bars are ± 1 standard error.

Table 2.6: ANOVA results for chlorophyll a concentrations by year, month and site.

Source	df	SS	F	P
Year	2	17.328	14.572	**0.002**
Month	1	2.984	5.019	0.055
Site	4	3.762	1.582	0.269
Year x Month	2	9.134	7.682	**0.014**
Year x Site	8	1.749	0.368	0.911
Month x Site	4	1.128	0.474	0.754
Residual	29	40.841		

TSS concentrations provide a measure of the amount of suspended inorganic and organic particles in the water which effect water clarity. There were no significant differences in TSS concentrations between year, month and site (Table 2.7). Mean January concentrations averaged across all sites and years of 9.271 ± 0.378 mg/L were similar to the mean May concentrations 7.937 ± 0.359mg/L (Table 2.2). Intermittent, elevated concentrations up to a factor

of 8 greater than the mean monthly values were observed at BXZ and LRN in January 2016 and May 2017, respectively (Figure 2.16).

Table 2.7: ANOVA results for TSS concentrations by year, month and site.

Source	df	SS	F	P
Year	2	246.335	0.497	0.626
Month	1	18.283	0.074	0.793
Site	4	944.391	0.953	0.482
Year x Month	2	684.975	1.383	0.305
Year x Site	8	2709.983	1.367	0.334
Month x Site	4	1397.036	1.410	0.314
Residual	29	7982.733		

Plankton: Abundance, Composition, Biomass and Indicators

Phytoplankton

Significant differences in phytoplankton community structure between years and site were observed based on cell counts from microscopy (Table 2.8). Pairwise comparisons between years, however, revealed no significant differences between the community in 2016 and the community in 2017 (P = 0.059) or 2018 (P = 0.302), and no significant differences between the community in 2017 and the community in 2018 (P = 0.074). This most likely reflects the weakly significant global effect for year in the PERMANOVA (i.e. P = 0.044).

Differences between sites were more complex. LFZ was significantly different to BXZ (P = 0.025) and BRN (P = 0.029), but not significantly different to LRN (P = 0.675) or LRS (P = 0.341). BXZ was not significantly different to BRN (P = 0.617) or LRN (P = 0.065) or LRS (P = 0.087). BRN was significantly different to LRN (P = 0.013) but was not significantly different to LRS (P = 0.070), and LRN was not significantly different to LRS (P = 0.843). These findings are consistent with the modelled circulation (Figures 2.4 and 2.12) and the patterns observed for nutrients, chl a, and indicate inshore sites within Boston and Louth Bay's (BXZ, BRN) generally differ from sites located offshore.

Table 2.8: PERMANOVA results for the phytoplankton community key functional groups (diatoms, dinoflagellates and other flagellates, in units of cells/L) by year, month and site.

Source	df	SS	Pseudo-F	P
Year	2	617.44	3.791	**0.043**
Month	1	59.851	0.735	0.456
Site	4	1641.5	5.039	**0.009**
Year x Month	2	97.524	0.599	0.624
Year x Site	8	409.00	0.628	0.779
Month x Site	4	451.53	1.386	0.296
Residuals	8	651.53		

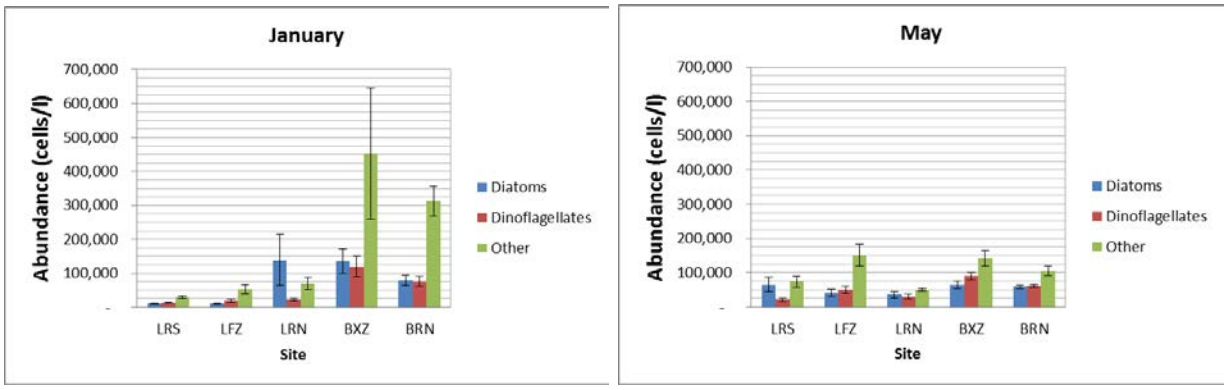

Figure 2.17: Mean abundances of diatoms, dinoflagellates and other flagellates (cells/L) at each site averaged over the 3-survey years for (left) January and right (May). Error bars are ± 1 standard error.

Three year mean total cell abundances in January ranged between 53,275 cells/L at LRS and 708,878 cells/L at BXZ, with total abundances at BXZ and BRN significantly greater than those measured at LRS and LFZ. Increases at BXZ and BRN were driven by an increase in cell abundances across each of the major taxonomic groups (Figure 2.17), particularly species belonging to the 'other' flagellates group; which were dominated by Prymnesiophytes, Cryptophytes and Prasinophytes. The observed total cell abundances ranged between a factor of 1 (LRS) to 14 (BRN) (mean ± se = 6.1 ± 1.9) greater than the mean total cell abundances (~50,000 cells/ L) previously reported for the region in January (Tanner and Volkman 2009, Middleton et al. 2013). Previously reported cell abundances for January (Tanner and Volkman 2009, Middleton et al. 2013) suggest these ratios were approximately equivalent (i.e. 1:1:1), with little spatial variation occurring across the region. With the exception of LRN, the previously reported 1:1 ratio largely holds for diatoms and dinoflagellates during January, 'others' dominated diatoms by about a factor of ~2.5 at offshore sites and up to factor of 3 at inshore sites (Fig 2.18).

Three year mean total cell abundances in May ranged between 115,552 cells/L at LRN and 294,868 cells/L at BXZ, with total abundances at BXZ and BRN significantly greater than those measured at LRS. Abundance increases observed at inshore sites were again driven by an increase in the abundance of species belonging to the dinoflagellates and 'other' flagellates groups (Figure 2.17). Observed total cell abundances are around a factor of 2 lower than the mean total cell abundances (~250,000 cells/L) reported for the region in Tanner and Volkman (2009), and on par with those reported by Middleton et al. (2013). However, both previous studies indicated a clear dominance of diatoms over dinoflagellates by up to a factor of 10 and diatoms to 'others' by factors of 2 to 4 during autumn. There was a clear shift from previously reported ratios in May, with ratios for diatoms to dinoflagellates decreasing from 3.4 at LRS to 0.71 at BXZ (Figure 2.18). Similarly, ratios for diatoms to 'others' decreased from 0.73 at LRS to 0.27 and BXZ in May.

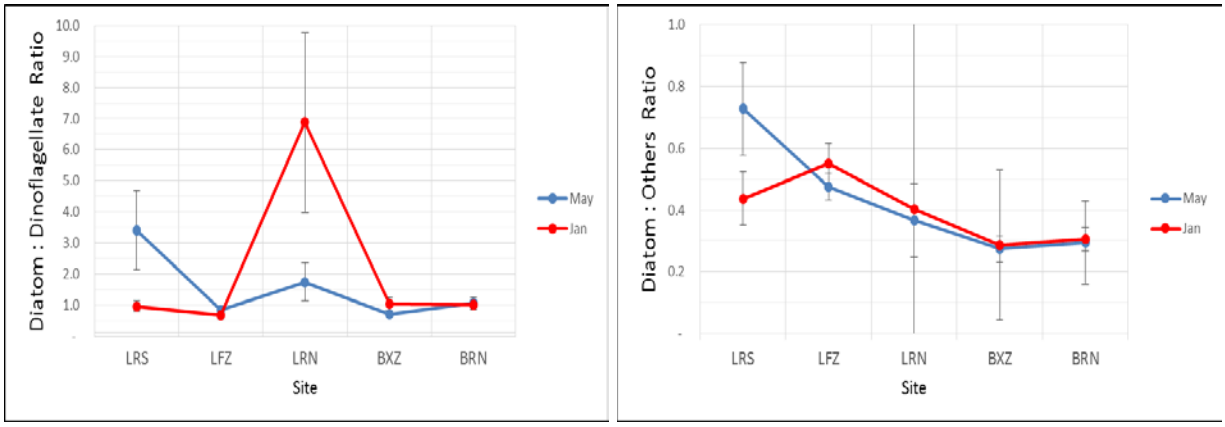

Figure 2.18: Mean abundance ratios showing the relative proportions of (left) Diatoms to Dinoflagellates and (right) Diatoms to 'Others' by site and month averaged over the 3-survey years. Error bars are ± 1 standard error. Note: Site LRN showed large variation in January and the y-axis has been adjusted to focus on the mean trends.

Harmful Algal Bloom Species

A total of 30 potentially harmful algal bloom species (HAB), including both toxic and non-toxic species (Tanner and Volkman 2009), were identified across the 3 survey years. Mean total HAB cell abundances averaged over the 3 survey years show an increase in the abundance of HAB cells in autumn relative to summer and at inshore sites (BXZ and BRN) and LFZ in both seasons (Figure 2.19). While most species were typically in low concentrations, there were dominant species by month and site (Tables 2.9 and 2.10). Dominant HAB species present during January included a mixture of diatom, dinoflagellate and other species. HAB species in May were dominated by dinoflagellates (i.e. *Dinophysis* species). Both the frequency of occurrence and number of HAB species were higher at inshore stations (BXZ and BRN) in both months. Identified species included several species associated with shellfish poisoning and fish kills (Tanner and Volkman 2009).

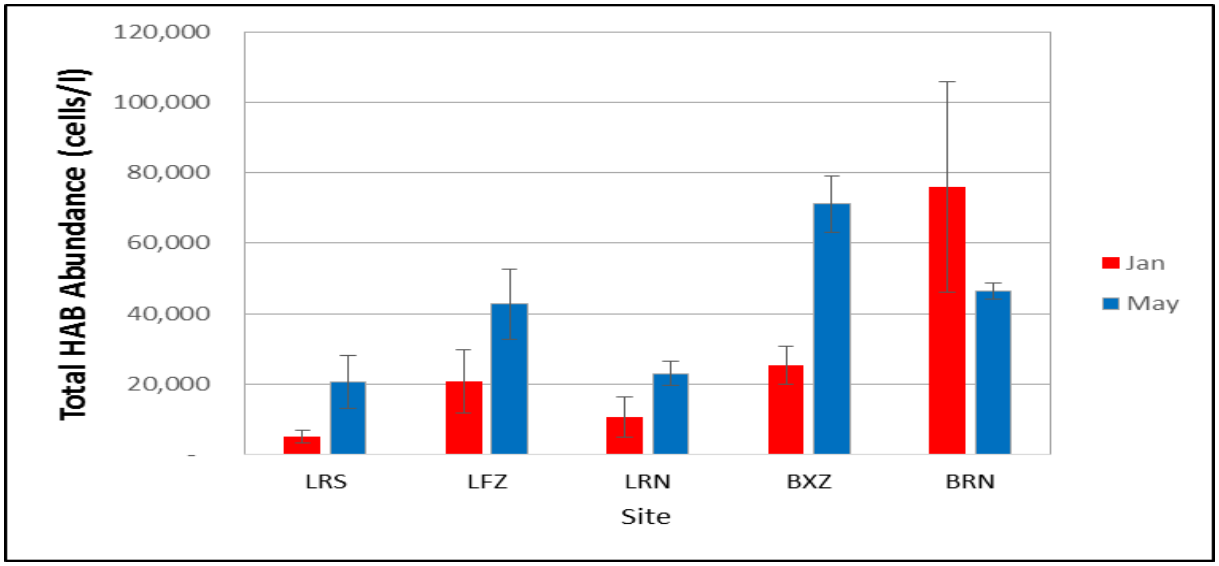

Figure 2.19: Mean abundance (cells/L) of HAB species at each site averaged over the 3-survey years for (left) January and right (May). Error bars are ± 1 standard error.

In January, HAB species with cell concentrations >10,000 cells/L were observed at all sites except LRS, with a maximum concentration of *Prymnesium patellifera* at 160,000 cells/L observed at BRN in 2016. This is an increase compared to the January trends presented in Tanner and Volkman (2009) where HAB species at concentrations >10,000 cells/L were typically observed to only occur between March and June. Across all years during May, multiple dinoflagellate HAB species with cell concentrations >10,000 cells/L were observed at all stations except for LRS (Tables 2.9 and 2.10).

Table 2.9: Dominant HAB species identified with cell concentrations >10,000 cells/L by site and month. Sites in bold type correspond with the maximum cell concentrations observed for that species.

Month	Genus	Species		Sites	Max. Abundance (cells/l)
January	Diatoms	*Pseudo-nitzschia*	*delicatissima*	**BXZ**	10,000
	Diatoms	*Pseudo-nitzschia*	*galaiae*	**BXZ**, BRN	19,000
	Dinoflagellates	*Karenia*	*papilionacea*	**BRN**	13,500
	Dinoflagellates	*Takayama*	*spp.*	**BXZ**	10,000
	Prymnesiophytes	*Prymnesium*	*patellifera*	LFZ, LRN, BXZ, **BRN**	160,000
	Other	*Heterosigma*	*akashiwo*	**LRN**, BRN	13,000
May	Diatoms	*Pseudo-nitzschia*	*brasiliana*	**LRS**	10,000
	Dinoflagellates	*Cochlodinium*	*spp.*	LRS, **LFZ**, LRN, BXZ, BRN	50,000
	Dinoflagellates	*Dinophysis*	*acuminata*	LFZ, LRN, BXZ, **BRN**	37,000
	Dinoflagellates	*Dinophysis*	*caudata*	LRS, LFZ, LRN, **BXZ**, BRN	22,000
	Dinoflagellates	*Dinophysis*	*truncata*	LRS, LFZ, LRN, **BXZ**, BRN	17,000

Table 2.10: HAB species frequency of occurrence by site and year.

Month	Site	Years present	No. of Species >10,000 cells/L
January	LRS	-	-
	LFZ	2016	1
	LRN	2016	2
	BXZ	2016, 2018	5
	BRN	2016, 2017, 2018	4
May	LRS	2018	3
	LFZ	2016, 2017, 2018	2
	LRN	2016, 2017, 2018	2
	BXZ	2016, 2017, 2018	4
	BRN	2016, 2017, 2018	3

Phytoplankton Pigments

Mean F_p values ranged from 0.17 ± 0.03 at LRS to 0.37 ± 0.04 at BXZ in January and 0.19 ± 0.13 at LRS to 0.43 ± 0.07 at BXZ in May (Figure 2.20). There were significant differences in F_p values concentrations between years and sites, and site was the most influential explanatory variable (Table 2.11). Pairwise comparisons showed F_p values averaged across all sites were greater in 2016 compared to 2017, with no significant difference between 2017 and 2018. F_p values at BXZ and BRN were significantly greater than those at LRS, LFZ, and LRN. These results are consistent with the changes observed in phytoplankton abundance and composition determined from microscopy.

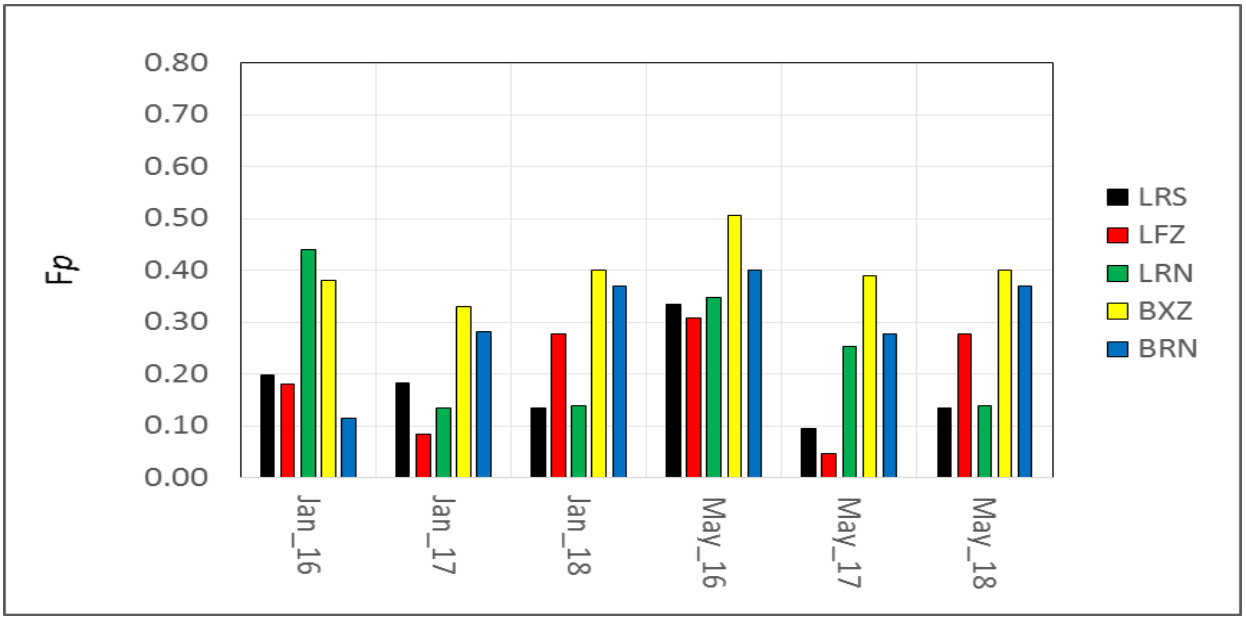

Figure 2.20: F_p ratio for sites, months and years.

Table 2.11: ANOVA results for F_p ratios by year, month and site.

Source	df	SS	F	P
Year	2	0.066	6.248	**0.023**
Month	1	0.013	2.525	0.151
Site	4	0.195	9.279	**0.004**
Year x Month	2	0.021	2.003	0.197
Year x Site	8	0.103	2.450	0.113
Month x Site	4	0.007	0.353	0.835
Residual	29	0.477		

Zooplankton Abundance

Zooplankton abundance was always higher in samples from the 64 µm mesh than from the 150 µm mesh net, by a factor of 2 to 5 (Figure 2.21). Relatively high abundances were observed at BXZ and BRN in all months of the study. The highest total abundance was observed at BRN (255,513 organisms/m^3) in May 2017, with high abundance also observed at BXZ (248,955 organisms/m^3) during this month. Abundances in samples from the 150 µm mesh net were ~4 to 8 times higher at BXZ and BRN than any other site. Total abundances at LRS and LFZ were relatively high during January 2018 (136,251 and 116,166 organisms/m^3, respectively).

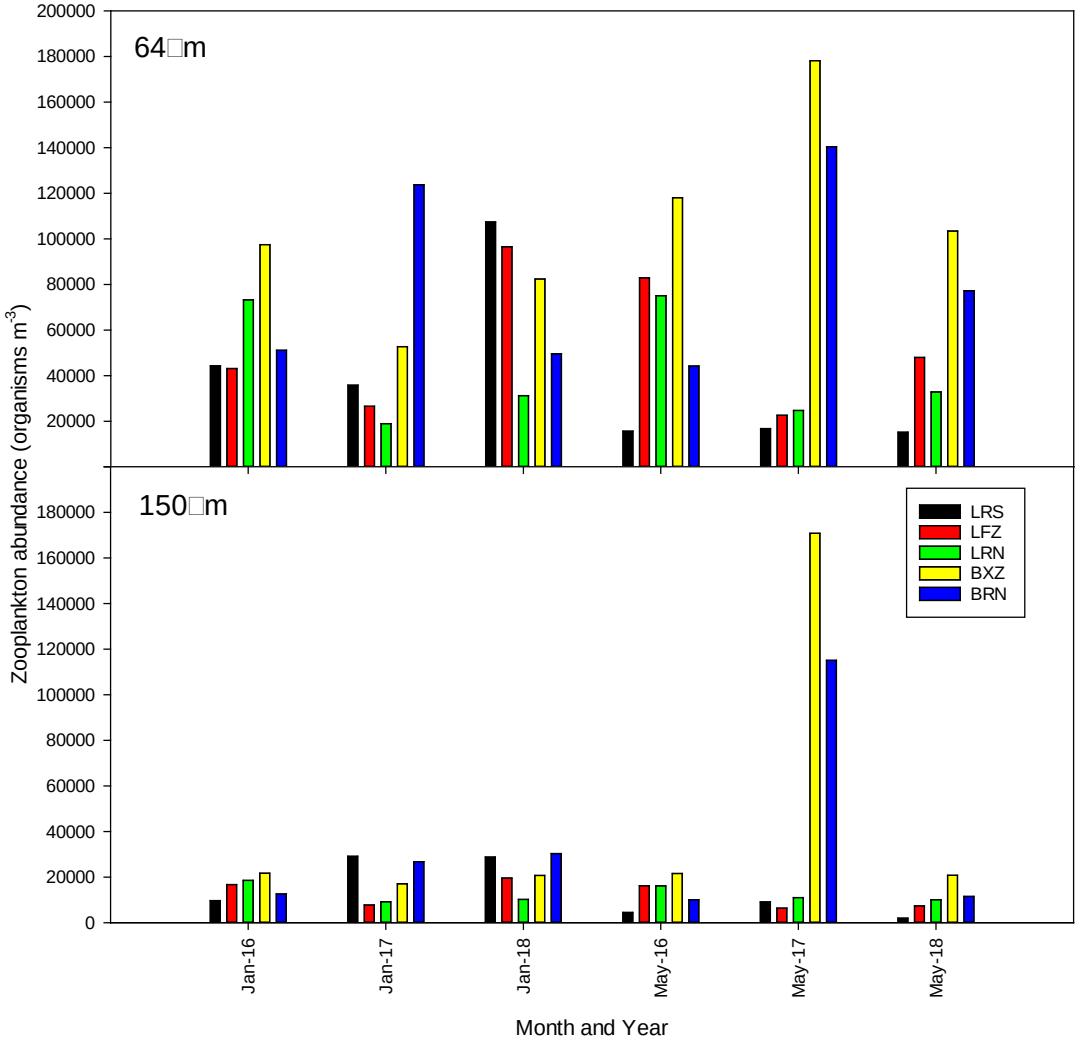

Figure 2.21: Zooplankton abundance (organisms m^{-3}) collected from the 64 µm and 150 µm mesh net.

Plankton Community Biomass

Figure 2.22 shows the amount and relative proportions of carbon biomass distributed among the key planktonic size classes. Generally, similar patterns of carbon biomass distribution among planktonic size classes were observed within sites, seasons (i.e. month) and years (Figure 2.22). For January, mean bacterial biomass averaged over 3 years ranged between 4.3 µg C/ L (LRS) and 9.3 µg C/ L (BRN). Phytoplankton biomass was dominated by picophytoplankton at LRS (13.0 µg C/ L) and LFZ (28.7 µg C/ L). Compared with LRS, phytoplankton biomass was higher across all size fractions at the other sites and was dominated by microphytoplankton at inshore

sites (e.g. 65.8 µg C/ L at BXZ). Zooplankton dominated the community biomass at LRS (107.2 µg C / L), where it was a factor of 2-3 times greater than that observed at other sites.

During May, mean bacterial biomass averaged over 3 years ranged between 8.0 µg C/ L (LRS) and 11.4 µg C/ L (BRN). The proportion of picophytoplankton present increased slightly offshore and ranged between 25.2 µg C/L (BXZ) and 33.1 µg C/ L (LRS). Spatially, sites LFZ, BXZ and BRN had more biomass in the nano- and microphytoplankton size classes relative to offshore sites. Microphytoplankton dominated the phytoplankton biomass at the inshore site BXZ (39.8 µg C/ L). Zooplankton contribution to the community biomass was greatest at LRN, BXZ and BRN, with a maximum mean biomass of 77.6 µg C / L at BXZ and minimum mean biomass of 11.2 µg C / L at LFZ.

There were significant differences in the community structure of the planktonic ecosystem between years, months and sites but no interactions (Table 2.12 and Figure 2.23). Pairwise comparisons indicated that the community in 2016 was significantly different to the community in 2017 (P = 0.012) and 2018 (P = 0.046), and the community in 2017 was significantly different to the community in 2018 (P = 0.002). Communities present in January were significantly different to those present in May (P = 0.009). Differences between sites were a little more complex. LFZ was significantly different to BXZ (P = 0.034) and BRN (P = 0.015), but not significantly different to LRN (P = 0.819) or LRS (P = 0.337). BXZ was not significantly different to BRN (P = 0.578) or LRN (P = 0.077), but was significantly different to LRS (P = 0.007). BRN was not significantly different to LRN (P = 0.063) but was significantly different to LRS (P = 0.038), and LRN was not significantly different to LRS (P = 0.615). These findings are consistent with the modelled circulation (Figures 2.4 and 2.12) and the general patterns observed for nutrients, chl a, phytoplankton community composition (Figures 2.14, 2.16, 2.17) and pigments (Figure 2.20).

The best explanation of the influence of environmental factors on variation in planktonic ecosystem structure came from a two variable model including NH_4^+ and NO_x, which had the lowest AIC value, and explained ~21% of variability in lower trophic ecosystem community structure (AIC = 124.4, R^2 = 0.207, Table 2.13). Changes in average NH_4^+ concentrations explained 65.4% of the model variation and 13.5% of total variation (dbRDA axis 1, Figure 2.24), while changes in average NO_x concentrations explained 34.6% of the model variation and 7.1% of the total variation (dbRDA axis 1).

Figure 2.22: The amount and relative contribution of carbon biomass distributed among the key autotrophic and heterotrophic planktonic size classes by site, month and year. (Top) Carbon contribution of each size class to the total biomass (µg C/L). (Bottom) Percentage contribution of each size class to the total biomass.

Table 2.12: PERMANOVA results for the planktonic community biomass composition by year, month and site.

Source	df	SS	Pseudo-F	P
Year	2	496.93	7.7952	**0.0006**
Month	1	186.37	5.8472	**0.0094**
Site	4	543.13	4.26	**0.0042**
Year x Month	2	27.207	0.42679	0.8181
Year x Site	8	192.2	0.75376	0.7248
Month x Site	4	256.15	2.0091	0.1012
Residuals	8	254.99		

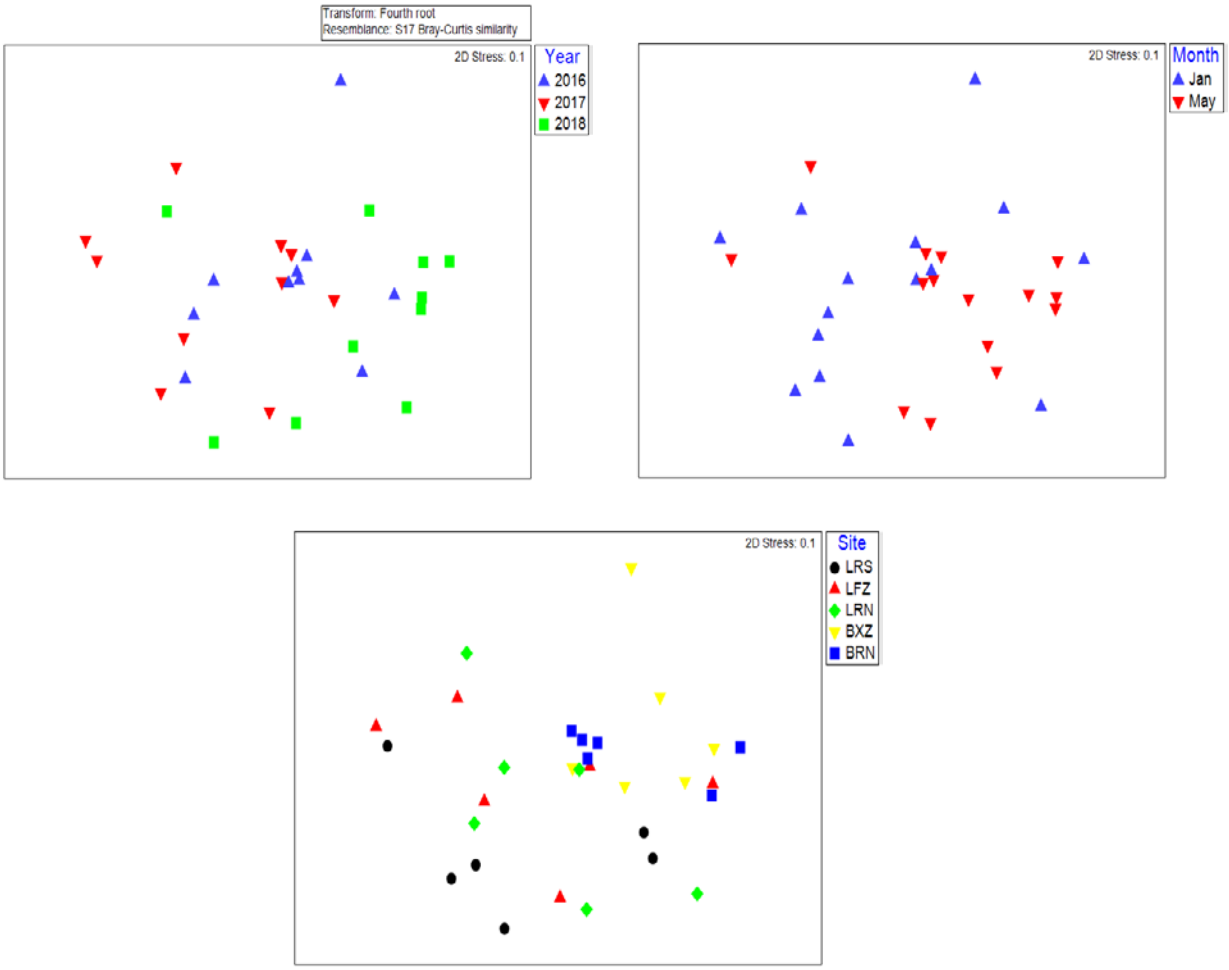

Figure 2.23: Non-metric multidimensional scaling (nMDS) plots showing separation in the community structure of the planktonic ecosystem by year, month and site.

Table 2.13: Overall best solutions for Distance Based Liner Model (DistLM) analyses of the influence of environmental variables of lower trophic ecosystem structure.

AIC	R^2	Variables
124.4	0.207	NO_x, NH_4
125.1	0.132	NH_4^+
125.2	0.184	NO_x, Si
125.4	0.233	NO_x, NH_4^+, Si
125.6	0.175	Temp, NH_4^+

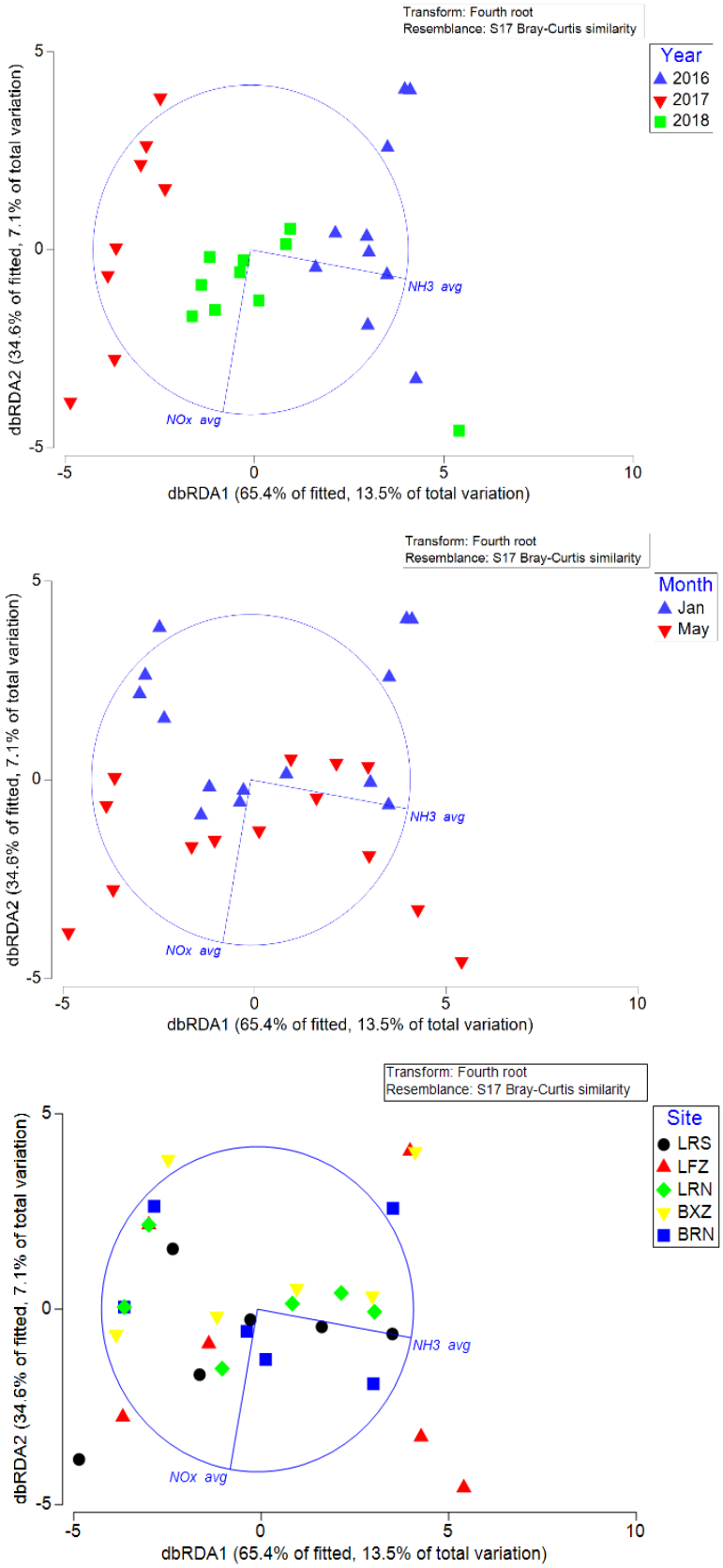

Figure 2.24: Distance based redundancy analysis (dbRDA) spell plot of planktonic community composition showing separation by year, month and site. Significant environmental factors influencing their distribution are shown by blue lines.

2.4. Summary and Conclusion

Results from the monitoring program showed spatial and temporal variation in the physical, chemical and biological parameters examined in the Boston Bay aquaculture zone and Lincoln (inner) sector of the Lincoln aquaculture zone. Observations are supported by modeling that shows physical variability influences the supply of natural nutrients from the shelf into the gulf and the connectivity and dispersal of anthropogenic nutrients across the region. Multiple indicators are used to assess the water quality trophic status of the system. Collectively, these suggest aquaculture may be having a significant impact on this component of the ecosystem in the physically connected inshore regions of Boston and Louth Bay.

The physical observations of currents, temperature, salinity and model results presented here are similar to those presented by earlier studies (Tanner and Volkman 2009, Teixeira 2010, Middleton et al. 2013, Doubell et al. 2015). In summary, strong semidiurnal tidal velocities are found (~0.4 m/s) and are modulated by the 28 day period dodge tide (Easton 1978). These are reproduced very well by the hydrodynamic model, with 91% of the observed variability explained by the model. The model reproduction of the dodge tide is important for two reasons. First, the associated shear dispersion is important for the accurate dispersal of heat, salt and biogeochemical scalars (e.g. nutrients, Figure 2.11)(Middleton and Doubell 2014). Second, an important function of the dodge tides is their role in modulating the dense saline gravitational outflow that occurs during autumn and winter. This outflow forms part of a gulf-scale clockwise gyre (~ 5cm/s) with a compensating inflow on the western side of the gulf (see Figure 2.5; Nunes and Lennon 1987, Nunes Vaz et al. 1990, Doubell et al. 2015). During summer, the exchange with the shelf is largely blocked (Petrusevics 1993, Nunes and Lennon 1987). The gulf-scale clockwise circulation also plays a key role in the prevention of any build-up of salt in the upper gulf due to evaporation and hence the annual (autumn) exchange of nutrients and organic material between shelf and gulf in autumn (Middleton et al. 2013). Simply, larger salt concentrations that might arise will be lowered through enhanced exchange with the shelf. This feedback mechanism acts to reduce any inter-annual variability of the circulation that might arise from climate or other mechanisms for change.

The low-pass filtered estimates of observed and model temperature and salinity support the inflow of water along the western side of Spencer Gulf in mid to late March (Nunes and Lennon 1987, Nunes Vaz et al. 1990, Middleton et al. 2013). The model results are very well correlated with temperature observations, with $r^2 > 0.8$. The monthly mean estimates of model currents support this, with northward currents after mid-March. We note that the monthly mean model currents

exhibit considerable spatial and inter-annual variability during January. Superimposed on the tidal and seasonal clock-wise flow are currents in the 3-10 day period weather-band. Observations and model results show the weather-band currents are forced in part by local winds and are much weaker (< 0.1 m/s) than the tides. The model does reproduce the observed weak current amplitudes, but not always specific wind-forced events.

The strong validation of the physical model underpins the biogeochemical model's ability to generally reproduce the magnitude and timing of observed NO_x, NH_4^+ and chl a concentrations (Figures 2.11 and 2.12). Differences between year's, months and sites are likely to be influenced by variability in the regional circulation (Figures 2.4) which modulates the supply and dispersal of natural and anthropogenic nutrients (Figures 2.12). Importantly, the coupled model reproduces the NO_x flux from the shelf into the gulf, and provides good predictions for NH_4^+, both of which are at their maximum in autumn in the LFZ during peak feed inputs (Middleton et al. 2013). The application and relevance of this nitrogen based model is supported by results from plankton community analysis (Figure 2.23), which indicated NH_4^+ and NO_x were the key environmental factors responsible for driving variations in planktonic ecosystem structure (Table 2.13). Hence, the model is useful for understanding the connectivity and dispersal of nutrients, the resultant phytoplankton biomass response (i.e. chl *a*), and the general space-time dynamics of nutrients and key water quality parameters at local and regional scales (Middleton et al. 2013, Doubell et al. 2015). Overall, the coupled physical-biogeochemical model provides a strong foundation for the future addition of important ecosystem components s (e.g. seagrass, macro-algae and shellfish) which may act as significant sinks of anthropogenic nutrients and experience growth or degradation as a result of addtional nutrient inputs.

Both spatial and temporal variation were detected in observed water quality variables. This is not surprising considering observations are limited to a snapshot (i.e. 1 water sample) taken in January and May of each year. Nonetheless, some general patterns consistent with both the seasonal circulation features and aquaculture activities were observed. NO_x concentrations were higher during May compared to January (Figure 2.14), consistent with reduced (enhanced) exchange between the shelf and Gulf in January (May), which is supported by the model results (e.g. Figures 2.4 & 2.12)(Middleton et al. 2013). NH_4^+ and PO_4^{3-} concentrations were greatest at LFZ (in the Lincoln aquaculture zone) during May (Figure 2.14), corresponding with the peak in nutrient emissions from aquaculture (Figure 2.12) (Fernandes et al. 2007). Modeling shows NH_4^+ at times approaches the ANZECC/ARMCANZ (2000) water quality guideline concentrations at LFZ (Figure 2.12), and is evident, albeit at reduced levels, at inshore sites (BXZ, BRN) but not

offshore at LRS. This supports the observations (Figure 2.14), modelled circulation features (Figure 2.4), and the generally well-mixed nature of the water column in the region (Figure 2.8).

Examining the observed nutrient concentrations and ratios showed nutrient limitation is likely to be key in limiting phytoplankton growth (Figure 2.15) (Tanner and Volkman 2009, Middleton et al 2013). Nutrients, phytoplankton biomass (chl *a*) and TSS concentrations (Figures 2.14 & 2.16, Table 2.2) were all generally in the range previously reported for the region (Tanner and Volkman 2009, Middleton et al 2013). However, in contrast to Tanner and Volkman (2009), spatial variation across the region was evident in nutrients and elevated chl a concentrations were observed at inshore stations (BXZ and BRN). Again, this is not surprising, since the models indicate connectivity between the aquaculture zones and inshore areas of Boston and Louth Bay, which are themselves characterized by reduced flushing compared to offshore waters (Middleton et al. 2013).

Several indicators used in this study showed a shift in the planktonic community structure and trophic status across the region. The change in trophic status from oligotrophic to mesotrophic at inshore sites indicated by the F_p ratio (Figure 2.20) (Claustre 1994) was associated with a shift in the microphytoplankton community composition away from diatoms to 'other' flagellated cells in January, and both dinoflagellates and 'others' in May, particularly at the inshore sites (Figures 2.17 and 2.18). Inshore sites also showed an increased presence and frequency of HAB species (Figure 2.20 and Tables 2.9 and 2.10). Further quantification of the carbon biomass across each of the major size and trophic components of the planktonic ecosystem (Figure 2.22) showed differences between sites, months and years (Figure 2.23), which were primarily driven by changes in nitrogen supply (Figure 2.24) and were associated with a shift from smaller picophytoplankton at offshore sites to larger nano- and micro-phytoplankton size fractions at inshore sites (BXZ, BRN) (Figure 2.22). Collectively, the observed shift in phytoplankton biomass from smaller to larger (nano- to microphytoplankton) phytoplankton size-fractions, changes in plankton community composition and food-web structure indicated by microscopy and phytoplankton pigments, and the increased presence harmful algal bloom species at inshore sites are consistent with changes expected under increasing nutrient loads (Howarth 2008, Glibert 2017). Again, this is not surprising considering the oceanographic connectivity between aquaculture activities, and the reduced flushing regions of Boston and Louth Bay (Middleton et al. 2013). However, this conclusion is based on a limited dataset (i.e. a total of six data points comprised of two sampling events per year, one in in summer and one in autumn).

It is recommended that pelagic monitoring be continued given the complexity in understanding the planktonic ecosystem response to nutrients supplied via natural processes and anthropogenic sources, particularly during late autumn (i.e. May) when the annual peak in nutrients supplied from shelf coincides with the peak in nutrients sourced from finfish (SBT+YTK) aquaculture. A more extensive, quantitative examination of historic phytoplankton cell ratios across each of the major taxonomic groups (Tanner and Volkman 2009, Middleton et al. 2013) to those presented here would be useful in understanding the extent of the observed shift away from a historically diatom dominated system and would be beneficial in monitoring future changes. As demonstrated, validation of the model using the collected data streams provides several benefits including a greater understanding of bio-physical couplings across a range of temporal and spatial scales and interpolation of the concentration of key water quality parameters in space and time. Subsequently, it is recommended the modelling be continued and regular updates of the model output, including the CarCap software provided to PIRSA F&A, to assist in planning and management decisions regarding the sustainable development of aquaculture.

Finally, several new indicators based on planktonic ecosystem composition for this region are developed and introduced in this report (e.g. phytoplankton taxonomic group abundance ratios, F_p ratio, and planktonic ecosystem carbon biomass). With regular monitoring this set of complimentary indicators can be used to quantitatively assess future changes in the region. Importantly, the new capability developed through this work to quantify plankton community carbon biomass across the major microbial and planktonic heterotrophic and autotrophic size classes has important implications for the future management of the system including: detecting shifts in food web and trophic structure in relation to the natural and anthropogenic supply of nutrients, improving carrying capacity estimates and the development of integrated multi-trophic aquaculture to mitigate single-species finfish aquaculture activities.

3. BENTHIC COMPONENT

The standard method used globally to detect impacts on the environment is the BACI (Before/After, Control/Impact) design (Green 1979) and its variations such as Beyond BACI (Underwood 1991, 1994). In order to determine whether an impact has occurred, the design requires multiple sites that are potentially disturbed and multiple sites that are not, each preferably sampled repeatedly over multiple times. As such, a zone environmental monitoring program will require multiple sites within the zone and outside the zone, sampled preferably on an annual basis or minimally biannually (as done here). This design will not only allow the determination of whether there has been a change in the "mean numbers" of the measured variable, but also whether the variance in the measured variable has changed over time.

The Benthic Infauna Monitoring program for the Lincoln aquaculture zone (inner sector) comprises four sampling sites in the area where tuna farming exists (within 0.1-2 km of a lease boundary), four sampling sites just outside the zone of tuna farming where effects on infauna would be expected to have diminished to background levels (Cheshire et al. 1996a, b), and two sets of four sampling sites well away from tuna farming to be used as 'controls' (Figure 3.1). A total of four control sites are located each to the north and south of the zone to ensure that they had not been directly impacted by aquaculture activities. The choice of these sites was somewhat subjective, as the closer they are to the farming zones the more likely they are to be impacted, while the further they are the more environmentally different they will be. Sampling in the Boston Bay aquaculture zone follows a similar pattern, with the exception that there were three sets of sampling sites away from the zone. The location of sites away from farming for the Boston Bay aquaculture zone (control sites) requires careful consideration. To the north at similar depth is the Louth Bay aquaculture zone, where there is mussel farming, similarly to the south is the Proper Bay aquaculture zone, also with mussel farming. Both of these areas are also affected by the influences of other coastal activities and discharges. These issues mean that there is no single suitable control site, and thus multiple control sites are required.

Field sampling was carried out in 2016 and 2018, during May when SBT feeding is at its peak. At each site, 8 replicate sediment samples were collected using a HAPS Bottom Corer with 67 mm internal diameter deployed from the *RV Ngerin*. Samples were immediately preserved in formalin, and transported back to the SA Aquatic Sciences Center for processing. Infauna were identified to the lowest taxonomic level possible, which varied between taxa, although for analysis, data was examined at the family level for consistency. Traditional infauna enumeration rather than the

DNA-based assays of indicator taxa was used. This is because in the compliance-based monitoring, the DNA-based assays were developed for a select set of infauna taxa that were indicative of organic enrichment (Loo et al. 2006). For zone level monitoring, enumerating the full infaunal assemblage allows broader spatial and temporal changes to be assessed.

The license-based environmental monitoring that had been used previously was based on a review and power analysis carried out by Madigan et al. (2001), where each compliance site is compared to eight associated control sites to determine if the compliance site is significantly different from the mean of the control sites. Species area curves were also used to determine that 8 core samples were the minimum required at each site to give a meaningful representation of the area. The sampling design given above is broadly based on the recommendations by Madigan et al. (2001).

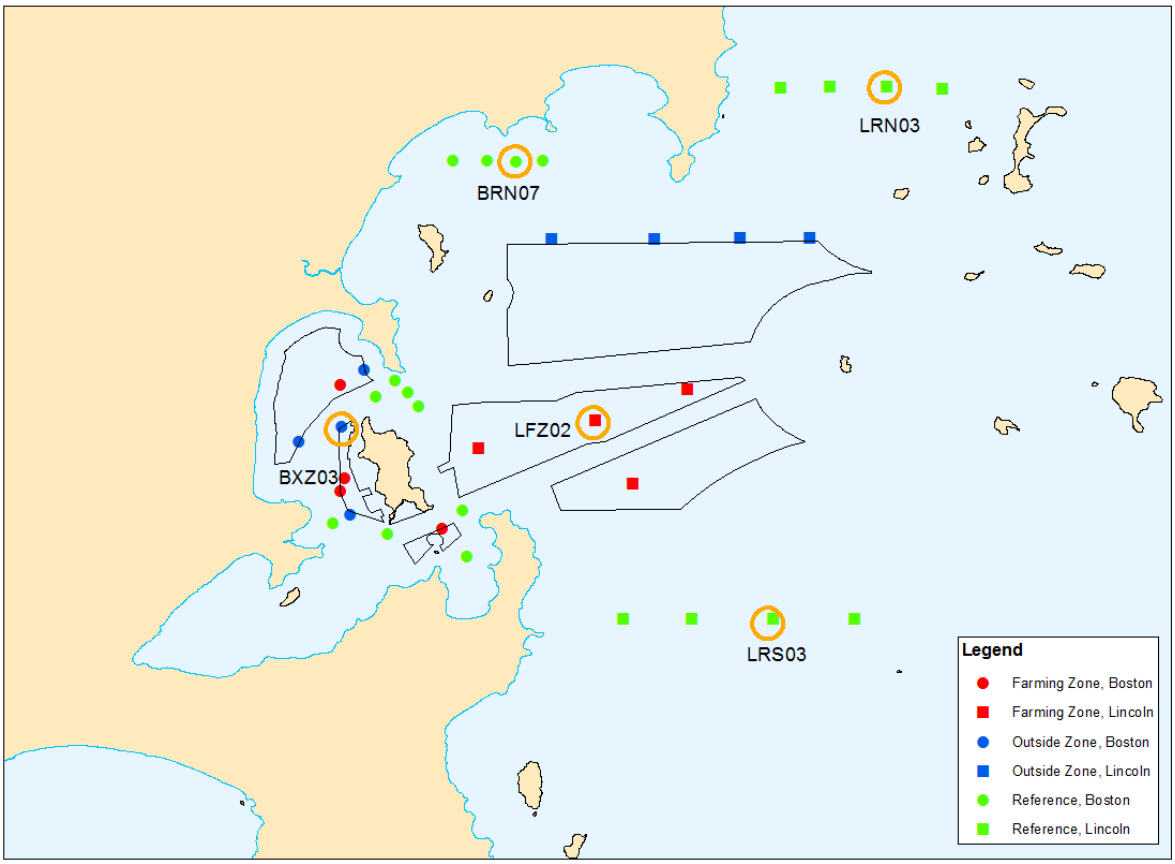

Figure 3.1: Location of infaunal sampling sites used in both 2016 and 2018. Black polygons indicate the Boston Bay and Lincoln (inner sector) aquaculture zones. Sites circled in orange are those used for the oceanography sampling described above.

3.1. Data analysis

Data were analysed for each year independently to focus on spatial differences in infaunal assemblages, and then jointly to examine temporal changes. Differences in infaunal assemblages between zones, proximity to aquaculture, and sites, were examined with PERMANOVA followed by Principal Coordinates Analysis (Anderson 2001, Anderson et al. 2008). Data were fourth root transformed to downweight the influence of abundant taxa, and resemblance matrices were calculated using the Bray-Curtis index to eliminate the influence of joint absences of taxa. 9999 permutations were undertaken under a reduced model to calculate significance levels. For individual year analyses, Zone and Proximity to aquaculture (within zone, on the boundary, control/reference) were treated as fixed factors, with groups of sites (e.g. north control, south control) being random and nested within the Zone by Proximity interaction, and individual sites also being random and nested within SiteGroup. For the between years analysis, year was added as an additional orthogonal and fixed factor. Taxonomic richness and total abundance were also analysed in a similar way, using univariate PERMANOVA. All analyses were carried out using the Primer 7.0.11 software package (Clarke and Gorley 2015), with the PERMANOVA+ add-on (Anderson et al. 2008).

3.2. Results

2016

In 2016, there was no detectable difference in the infaunal assemblage between the two aquaculture zones, or due to proximity to aquaculture (Table 3.1). There were, however, differences due to SiteGroup (i.e. the different sets of reference sites in each zone differed), and between individual sites within each SiteGroup. Pairwise tests showed a difference between the Boston South and Boston Far North reference sites, as well as between the Lincoln North and Lincoln South sites. Although not significant, the principal coordinates plot does show some tendency for separation between the Boston and Lincoln zones (Figure 3.2). If we look at just the Lincoln zone, there is little overlap between the north and south reference samples, and the differences are driven by differences in abundance of a number of primarily polychaete families (Figure 3.3). There is also little overlap between the Boston reference far north and south samples, although in this case the difference is primarily driven by higher calanoid copepod abundance in the far north (Figure 3.3). For both total infaunal abundance and taxon richness,

there were no detectable differences between any of the factors considered, except between individual sites (Table 3.2).

Table 3.1: PERMANOVA results for infaunal assemblage composition in 2016

Source	df	SS	Pseudo-F	P
Zone (Z)	1	29734	2.3434	0.0968
Proximity (P)	2	20182	0.79528	0.6377
Z x P	2	19144	0.75438	0.6687
SiteGroup(Z x P)	3	38066	2.4982	**0.0001**
Site(SiteGroup(Z x P))	27	1.37E+05	3.3289	**0.0001**
Residual	252	3.84E+05		

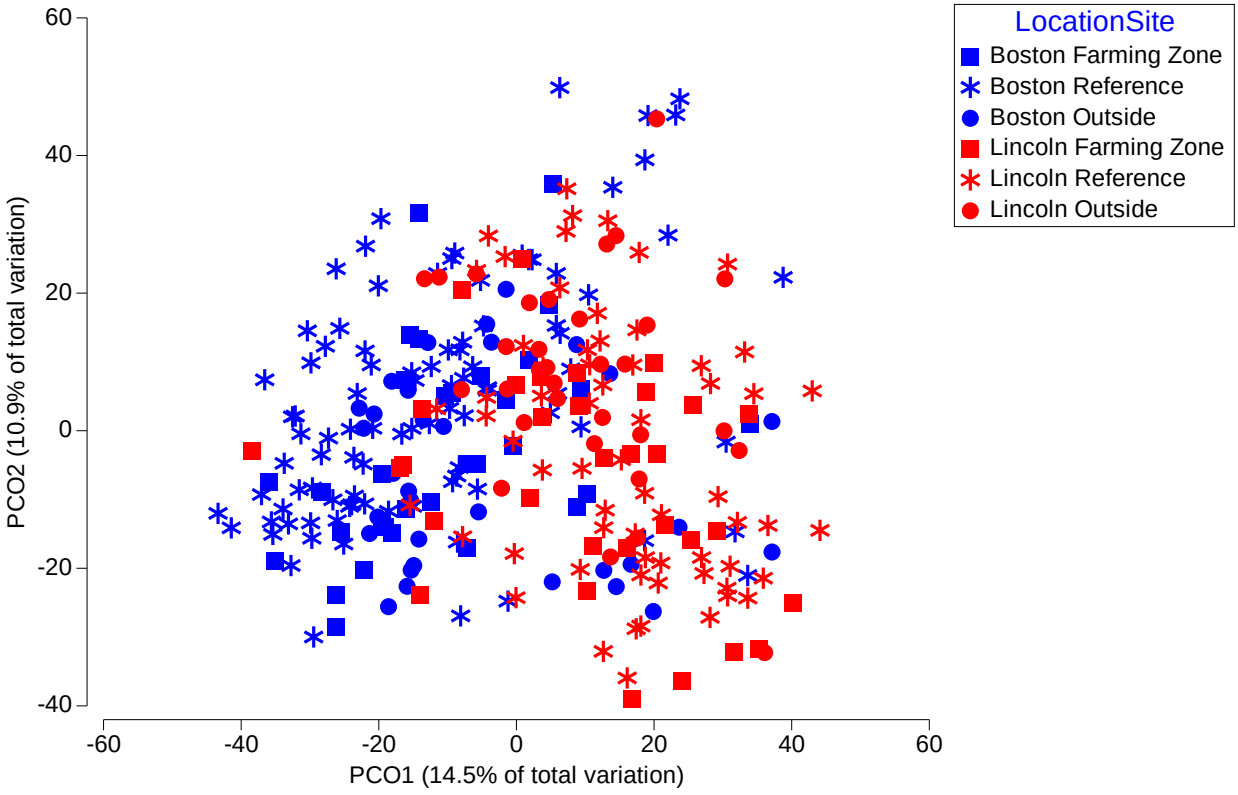

Figure 3.2: Principal coordinates plot of 2016 infaunal assemblage composition, showing some separation between Boston Bay sites (blue) and Lincoln sites (red).

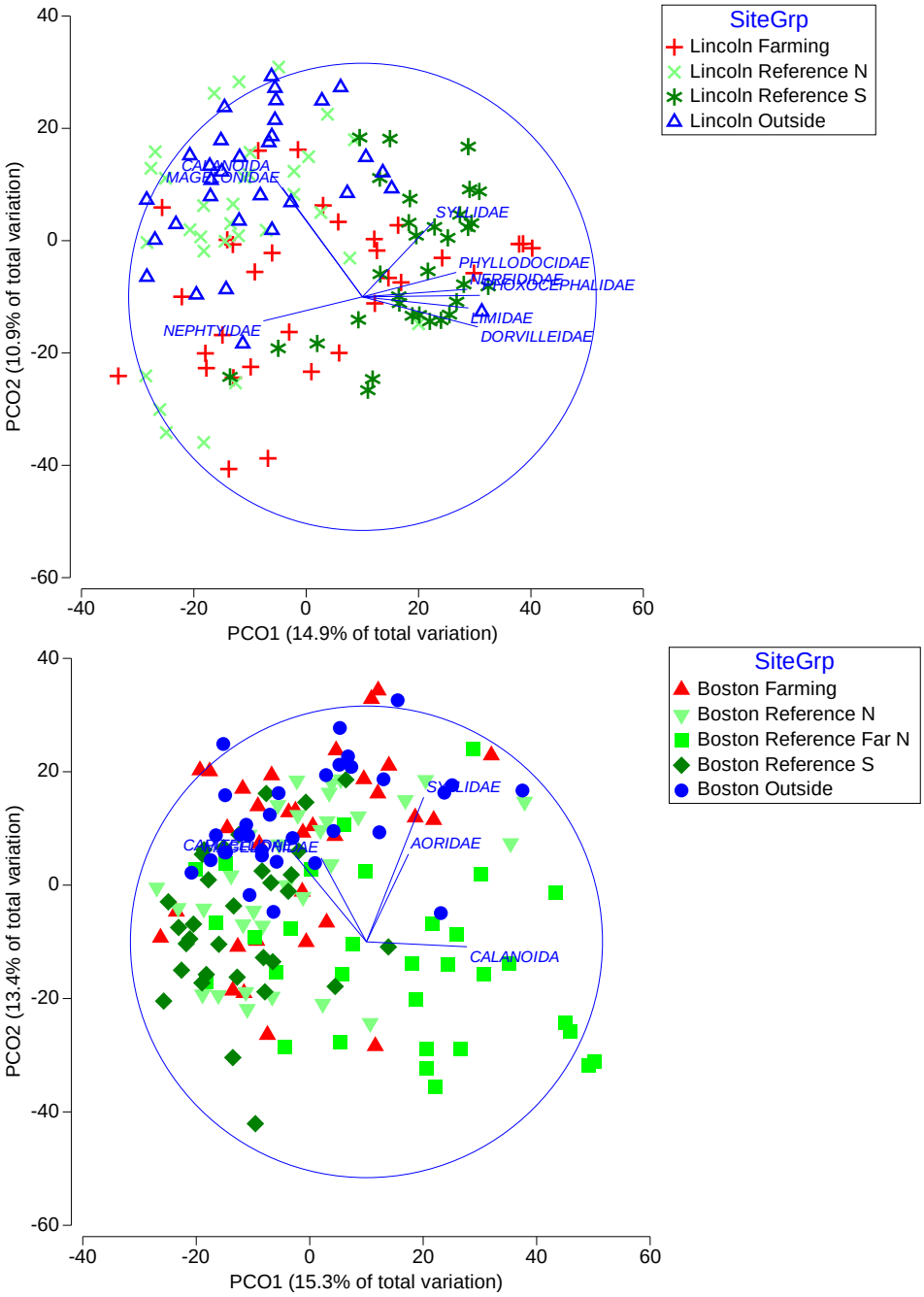

Figure 3.3: Principal coordinates plots for 2016 Lincoln (above) and Boston Bay (below) samples separately. Blue lines indicate taxa that have a Pearson correlation >0.4 with the axes, and which thus have substantially different abundances between samples that differ in the direction of the line. From the bottom, these taxa for the top panel are: Nephtyidae, Magelonidae, Calinoida, Syllidae, Phyllodocidae, Nereididae, Phoxocephalidae, Limidae and Dorvilleidae. For the bottom panel, they are: Magelonidae, Capitellidae, Syllidae, Aoridae and Calanoida. The blue circle indicates a correlation of 1.

Table 3.2: PERMANOVA results for total infaunal abundance and taxonomic richness in 2016.

		Total Abundance			Taxonomic Richness		
Source	**df**	**SS**	**Pseudo-F**	**P**	**SS**	**Pseudo-F**	**P**
Zone (Z)	1	145.15	0.70004	0.4665	84.026	0.93796	0.3964
Proximity (P)	2	537.79	1.2968	0.2967	108.38	0.60492	0.5482
Z x P	2	344.66	0.83113	0.495	259.93	1.4508	0.3324
SiteGroup(Z x P)	3	622.04	0.66775	0.5704	268.75	1.9453	0.1492
Site(SiteGroup(Z x P))	27	8383.9	5.5961	**0.0001**	1243.4	6.2473	**0.0001**
Residual	252	13983			1857.6		

2018

As with 2016, the only differences in infaunal assemblages in 2018 were between SiteGroups and Sites (Table 3.3). However, in this year, pairwise tests showed that only the Lincoln reference sites differed, and that the Boston reference sites did not differ from each other. Again, although not significant, the principal coordinates plot does show some tendency for separation between the Boston and Lincoln zones (Figure 3.4). If we look at just the Lincoln zone, there is again little overlap between the north and south reference samples, and the differences are driven by differences in abundance of a small number of polychaete families (Figure 3.5). In this case, there is substantial overlap between the Boston reference far north and south samples. For both total infaunal abundance and taxon richness, there were no detectable differences between any of the factors considered, except between individual sites (Table 3.4), as per 2016.

Table 3.3: PERMANOVA results for infaunal assemblage composition in 2018.

Source	**df**	**SS**	**Pseudo-F**	**P**
Zone (Z)	1	33066	2.0321	0.1482
Proximity (P)	2	17483	0.5372	0.8326
Z x P	2	19907	0.61171	0.8142
SiteGroup(Z x P)	3	48816	2.4466	**0.0007**
Site(SiteGroup(Z x P))	27	1.80E+05	3.4153	**0.0001**
Residual	252	4.91E+05		

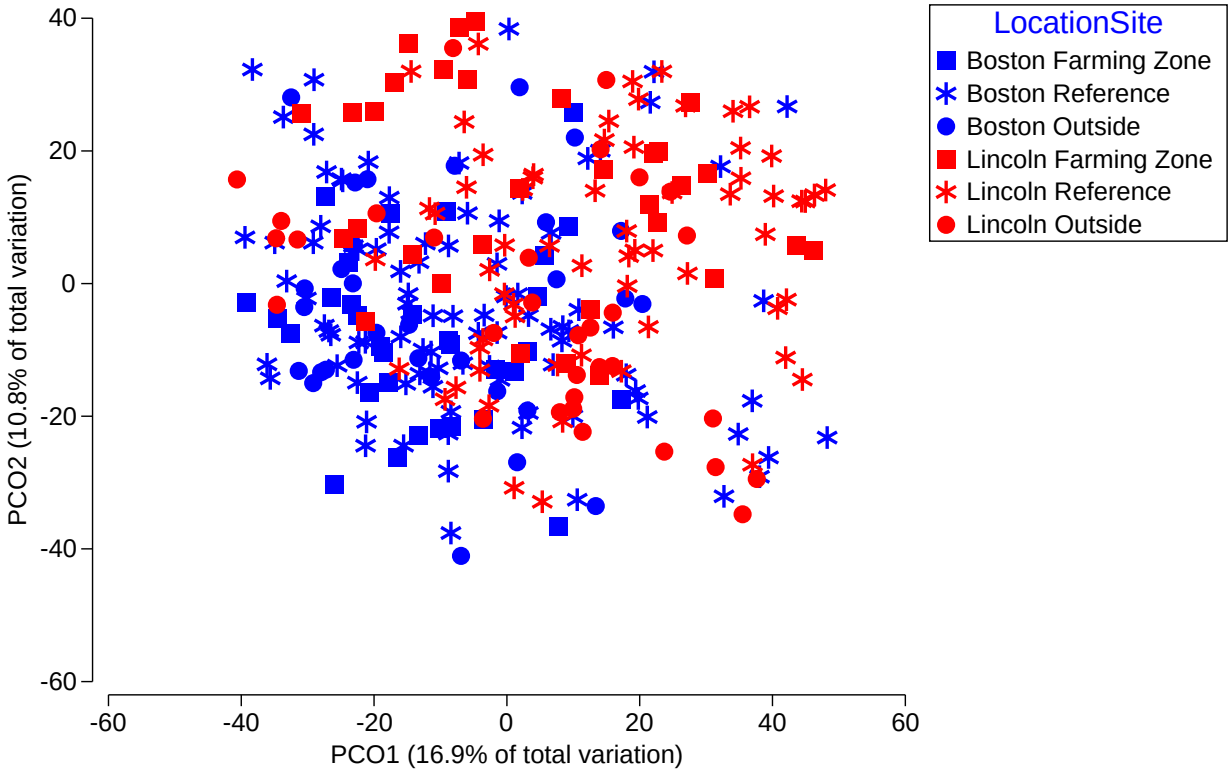

Figure 3.4: Principal coordinates plot of 2018 infaunal assemblage composition, showing some separation between Boston Bay sites (blue) and Lincoln sites (red).

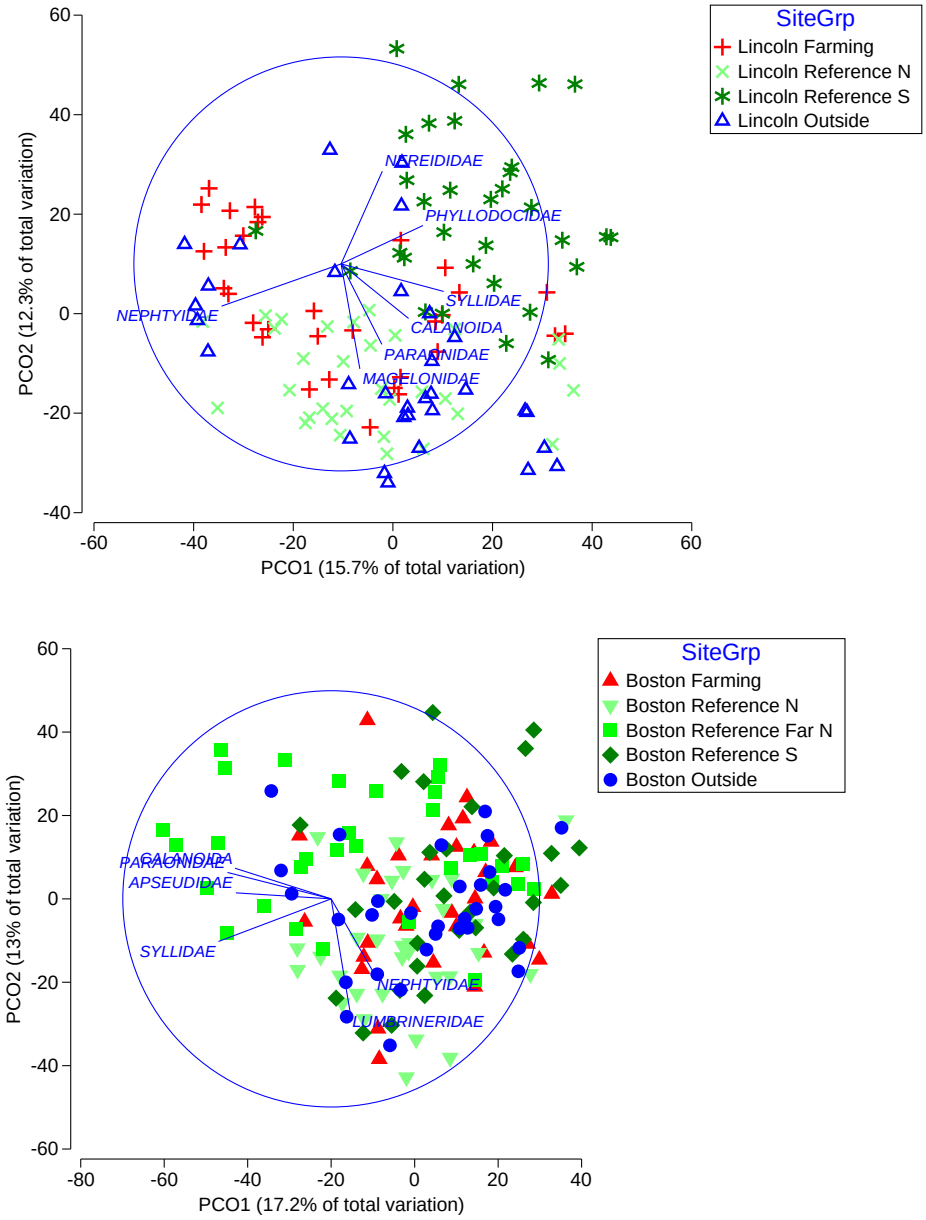

Figure 3.5: Principal coordinates plots for 2018 Lincoln (above) and Boston Bay (below) samples separately. Blue lines indicate taxa that have a Pearson correlation >0.4 with the axes, and which thus have substantially different abundances between samples that differ in the direction of the line. From the bottom, these taxa for the top panel are: Nephtyidae, Nereididae, Phyllodocidae, Syllidae, Calinoida, Paraonidae and Magelonidae. For the bottom panel, they are: Syllidae, Apseudidae, Paraonidae, Calanoida, Nephtyidae and Lumbrineridae. The blue circle indicates a correlation of 1.

Table 3.4: PERMANOVA results for total infaunal abundance and taxonomic richness in 2016.

		Total Abundance			Taxonomic Richness		
Source	**df**	**SS**	**Pseudo-F**	**P**	**SS**	**Pseudo-F**	**P**
Zone (Z)	1	47.449	0.49071	0.5507	30.19	0.66586	0.4828
Proximity (P)	2	210.32	1.0876	0.4079	10.033	0.11064	0.8003
Z x P	2	510.09	2.6377	0.1843	0.50758	0.005597	0.9835
SiteGroup(Z x P)	3	290.08	0.30279	0.8216	136.02	1.3142	0.294
Site(SiteGroup(Z x P))	27	8622.4	3.9753	**0.0001**	931.53	5.6388	**0.0001**
Residual	252	20244			1541.9		

Between Years

For the between years analysis, there was a significant interaction between year and both individual sites and proximity to aquaculture (Table 3.5). This result indicates that there were changes over time, but that they were not consistent between different levels of these two factors. This analysis also showed a zone effect, indicating differences between the Boston Bay and Lincoln zones. Consequently, the analysis was repeated for each zone individually. For the Lincoln zone, there was again an interaction between year and site, along with the SiteGroup effect (Table 3.6) that was found in the individual year analyses presented above. The former indicates that while there are temporal changes at the smallest spatial scale considered in the study (between sites within a site group), these changes were not consistent at larger spatial scales. The pattern was more complicated for Boston Bay, with a year by proximity effect also found (Table 3.6). Pairwise tests indicated that the only difference between years was for the outside group (i.e. those sites just outside the boundary of the zone), although there is no indication in the data that this might be due to these sites being affected by aquaculture in one year but not the other. The greater complexity of these interactions mean that they do not show up clearly on the principal coordinates plots, especially as the variation associated with them is small compared to the variation associated with the larger-scale spatial changes, and these are thus not presented. For both total infaunal abundance and taxonomic richness, there was also a significant year by site interaction, again indicating temporal changes at the smaller spatial scales examined that are not consistent at the larger scales (Table 3.7).

Table 3.5: PERMANOVA results for infaunal assemblage composition in 2016 and 2018.

Source	df	SS	Pseudo-F	P
Year (Y)	1	42021	8.2733	**0.0136**
Zone (Z)	1	58602	2.1782	0.1093
Proximity (P)	2	30723	0.57096	0.8576
Y x Z	1	11290	2.2228	0.1539
Y x P	2	10596	1.0431	0.4528
Z x P	2	33345	0.61969	0.7909
SiteGroup(Z x P)	3	80713	3.0084	**0.0001**
Y x Z x P	2	9322	0.91769	0.5245
Site(SiteGroup(Z x P))	27	2.41E+05	4.5778	**0.0001**
Y x SiteGroup(Z x P)	3	15237	1.2827	0.1292
Y x Site(SiteGroup(Z x P))	27	1.07E+05	2.0269	**0.0001**
Residual	504	9.85E+05		

Table 3.6: PERMANOVA results for between year comparisons for individual aquaculture zones.

	Lincoln				Boston Bay			
Source	**df**	**SS**	**Pseudo-F**	**P**	**df**	**SS**	**Pseudo-F**	**P**
Year (Y)	1	30701	2.8027	0.2333	1	22320	10.422	**0.0242**
Proximity (P)	2	43096	0.56486	1	2	21004	0.49346	0.9037
SiteGroup(P)	1	38147	5.2238	**0.0001**	2	42566	2.0752	**0.0232**
Y x P	2	9088.4	0.41484	0.843	2	11001	2.5685	0.0852
Site(SiteGroup(P))	12	87630	3.3504	**0.0001**	15	1.54E+05	5.7851	**0.0001**
Y x SiteGroup(P)	1	10954	2.078	**0.0292**	2	4283.1	0.73581	0.7824
Y x Site(SiteGroup(P))	12	63257	2.4185	**0.0001**	15	43657	1.6418	**0.0001**
Residual	224	4.88E+05	2.8027	0.2333	280	4.96E+05		

Table 3.7: PERMANOVA results for total infaunal abundance and taxonomic richness for both years combined.

		Total Abundance			Taxonomic Richness		
Source	**df**	**SS**	**Pseudo-F**	**P**	**SS**	**Pseudo-F**	**P**
Year (Y)	1	389.63	6.55	0.0824	304.02	13.022	**0.0336**
Zone (Z)	1	178.78	0.7354	0.4283	107.08	0.96779	0.3913
Proximity (P)	2	707.89	1.4559	0.289	90.456	0.40876	0.7073
Y x Z	1	13.173	0.22144	0.6695	6.6437	0.28456	0.641
Y x P	2	38.209	0.32116	0.7507	27.062	0.57956	0.6177
Z x P	2	8.415	0.017307	0.9883	121.14	0.54741	0.6191
SiteGroup(Z x P)	3	729.33	0.60307	0.6263	331.94	1.8887	0.1598
Y x Z x P	2	845.58	7.1075	0.0672	138.24	2.9606	0.1943
Site(SiteGroup(Z x P))	27	10884	5.9378	**0.0001**	1581.7	8.7015	**0.0001**
Y x SiteGroup(Z x P)	3	178.46	0.26279	0.8474	70.042	1.0674	0.382
Y x Site(SiteGroup(Z x P))	27	6111.7	3.3342	**0.0001**	590.58	3.249	**0.0001**
Residual	504	34217			3393.1		

3.3. Discussion

While both spatial and temporal variation were detected in the infaunal assemblages in the Boston Bay and Lincoln (inner) aquaculture zones, there were no differences detected that were consistent with aquaculture having a significant impact on this component of the ecosystem. Instead, there were differences between groups of reference sites in both zones, consistent with a north-south gradient in infaunal assemblages. A similar result was found in an earlier combined analysis of tuna and finfish environmental monitoring program data that included all samples collected between 2005 and 2014 (Tanner et al. 2017). Given changes in wave exposure and other environmental parameters between the different groups of reference sites, it is not surprising to find differences in their infaunal assemblages. It is perhaps more surprising that there were no differences between the Boston Bay and Lincoln aquaculture zones, although this again reflects

the earlier temporal analysis of the TEMP and FEMP data (Tanner et al. 2017). With Boston Bay sites being in shallower and more sheltered locations than the Lincoln sites, you would expect to see differences in sediment composition and thus infaunal assemblages. However, with some of the Boston Bay sites being more exposed than others, and some of the Lincoln sites being more inshore, it appears that both zones may have overlapping gradients, as supported by the principal coordinates analysis of the full data set for each of 2016 and 2018.

Unfortunately, it is not possible to combine the data presented here with this earlier data, as the current results are based on full enumeration of the infaunal assemblage using traditional manual sorting and taxonomic classification, while the earlier results are based on quantitative analysis of DNA from a select subset of taxa known to be indicators of organic enrichment (Loo et al. 2006, Loo et al. 2010). Consequently, we cannot determine if the apparent cyclical change over time documented for the Lincoln zone has continued. However, the fact that differences between 2016 and 2018 appear to be restricted to the smallest spatial scale studied here suggests that there has been at least a 2 year hiatus in this cycle. In interpreting these changes, it should also be borne in mind that in both years, there was considerable variability at the smallest spatial scale of sampling. Thus it is possible that what appears as temporal variability in the between years analysis is actually spatial variability, as it is likely that the exact sites differed by a few 10's of meters between years.

Assessment of infaunal assemblages has been a key component of environmental monitoring for the tuna and marine finfish aquaculture industries in South Australia since ~2001 (Loo et al. 2006, Loo et al. 2010). During this time, there have only been a few isolated incidences of an impact being detected on individual leases, and in those cases subsequent investigations determined that the lease boundaries had been incorrectly located, and thus compliance site sampling which was supposed to be 150m outside the lease actually took place inside the production area, where impacts are expected to be higher. Consequently, under current management and operational arrangements, and with an allowable zone of impact extending to 150m outside lease boundaries, the substantial body of monitoring that has been undertaken suggests that tuna and yellowtail kingfish aquaculture will not have a detectable effect on infaunal assemblages. It is thus recommended that infaunal monitoring be scaled back, and that resources are instead reallocated to examine other components of the environment that are at risk of being impacted by aquaculture, but which have so far received little attention. Thus instead of annually, as has occurred for most of this century so far, or every two years, as in this latest study, assessment of infaunal assemblages every five years is likely to be adequate. It should be stressed, however,

that this recommendation only holds under current arrangements. If there is appreciable change in the manner of farming (e.g. greater intensification), or change in the location of farming (especially if undertaken in more sheltered areas), then infaunal monitoring will still likely be required on a more frequent basis.

4. CONCLUSION

Collectively, the monitoring program and modelling suggest that aquaculture may be having a significant impact on the pelagic component of the ecosystem in the physically connected inshore regions of Boston and Louth Bay. The physical observations of currents, temperature and salinity, and the model results, are generally consistent with those presented by earlier studies, and show the inflow of water along the western side of Spencer Gulf in mid to late March.

The biogeochemical model generally reproduces the magnitude and timing of observed NO_x, NH_4^+ and chl a concentrations, the first two of which were shown to be the key environmental factors responsible for driving variations in planktonic ecosystem structure. Nutrients, phytoplankton biomass (chl a) and TSS concentrations were all generally in the range previously reported for the region.

Several indicators showed a shift in the planktonic community structure and trophic status in the region, including a reduction in the dominance of diatoms, phytoplankton community pigment compositions reflective of additional nutrient inputs and mesotrophic conditions at the inshore sites, along with an increased presence and frequency of HAB species at the inshore sites. In general, phytoplankton biomass levels also increased and shifted from smaller picophytoplankton at offshore sites to larger nano- and micro-phytoplankton size fractions at inshore sites.

Collectively, the observed changes in plankton community structure are consistent with changes expected under increasing nutrient loads, although with only six sets of samples, this is not conclusive, and the monitoring is continuing through 2020-2022 to assess whether the observed trends continue. A more extensive examination and comparison of historic diatom to dinoflagellate, and diatom to ‘others’ ratios to those presented here, and across a broader region (e.g. at IMOS sites), would be beneficial as it would provide a more quantitative assessment of the spatial extent of the observed shift and the potential role of climate change (if any) on the region.

While there was evidence of potential aquaculture impacts on the pelagic environment, no such impacts were detected in the infaunal data. In both 2016 and 2018, there was significant small-scale variation between sites, as well as larger scale geographic variation, but the farming zone sites all fell within the range of variation seen at the reference sites. In addition, there was no evidence in the temporal analysis of the previous TEMP and FEMP data to suggest any long-term changes in infaunal assemblages associated with aquaculture. As such, it is recommended that

infaunal monitoring be scaled back, and occur on a less frequent basis, provided that the farming systems generally remain the same as they were during the period of this study.

Given the indications that aquaculture may be having some effect on the ecosystem, the 2019-2023 AEMP will undertake more detailed investigations into the fate and consequences of the nutrients being added to the system. In particular, how these nutrients influence the local seagrass meadows will be examined. The status of seagrass beds inside and outside the modelled nutrient plumes will be examined in 2020 and 2022, and a suite of biomarkers utilized to determine if these seagrasses, or their epiphytes, are utilizing aquaculture derived nutrients. In combination, these studies will enable us to determine if aquaculture is having a sustained negative impact on a key ecosystem asset.

REFERENCES

Anderson, M. J. 2001. A new method for non-parametric multivariate analysis of variance. Austral Ecology **26**:32-46.

Anderson, M. J., R. N. Gorley, and K. R. Clarke. 2008. PERMANOVA+ for PRIMER: Guide to software and statistical methods. PRIMER-E, Plymouth, UK.

ANZECC/ARMCANZ. 2000. Australian and New Zealand guidelines for fresh and marine water quality. Australian and New Zealand Environment and Conservation Council and Agriculture and Resource Management Council of Australia and New Zealand, Canberra:1-103.

APHA-AWWA-WPCF. 1998. Standard methods for the examination of water. Sewage and Industrial Waste. American Public Health Association, Washington, DC.

Azam, F., and F. Malfatti. 2007. Microbial structuring of marine ecosystems. Nature Reviews Microbiology **5**:782.

Bode, A., M. T. Alvarez-Ossorio, and N. Gonzalez. 1998. Estimations of meso-zooplankton biomass in a coastal upwelling area off NW Spain. Journal of Plankton Research **20**:1005-1014.

Cheshire, A., G. Westphalen, T. Kildea, A. Smart, and S. Clarke. 1996a. Investigating the environmental effects of sea-cage tuna farming. I. Methodology for investigating seafloor souring. University of Adelaide, Adelaide.

Cheshire, A., G. Westphalen, A. Smart, and S. Clarke. 1996b. Investigating the environmental effects of sea-cage tuna farming. II. The effects of sea-cages. University of Adelaide, Adelaide.

Clarke, K. R., and R. N. Gorley. 2015. PRIMER v7: User manual/tutorial. PRIMER-E, Plymouth.

Claustre, H. 1994. The trophic status of various oceanic provinces as revealed by phytoplankton pigment signatures. Limnology and Oceanography **39**:1206-1210.

Cloern, J. E. 2001. Our evolving conceptual model of the coastal eutrophication problem. Marine Ecology-Progress Series **210**:223-253.

Doubell, M. J., C. E. James, and J. F. Middleton. 2015. Modelling of oceanographic variables for the development of finfish aquaculture in Spencer Gulf. SARDI Publication No. F2014/000740-1. SARDI Research Report Series No. 830. , South Australian Research and Development Institute (Aquatic Sciences), Adelaide. .

Easton, A. 1978. A reappraisal of the tides in Spencer Gulf, South Australia. Marine and Freshwater Research **29**:467-477.

Econsearch. 2018. The economic contribution of aquaculture in the South Australian state and regional economies, 2016/7. A report to PIRSA Fisheries and Aquaculture. Adelaide.

Erofeeva, G., and L. Egbert. 2014. TPXO8-ATLAS, v1. Oregon State University, College of Earth, Ocean, and Atmospheric Sciences, accessed 11 July 2016.

Fennel, K., J. Wilkin, J. Levin, J. Moisan, J. O'Reilly, and D. Haidvogel. 2006. Nitrogen cycling in the Middle Atlantic Bight: Results from a three-dimensional model and implications for the North Atlantic nitrogen budget. Global Biogeochemical Cycles **20**.

Fernandes, M., M. Angove, T. Sedawie, and A. Cheshire. 2007. Dissolved nutrient release from solid wastes of southern bluefin tuna (*Thunnus maccoyii*, Castelnau) aquaculture. Aquaculture Research **38**:388-397.

Fernandes, M., and J. Tanner. 2008. Modelling of nitrogen loads from the farming of yellowtail kingfish Seriola lalandi (Valenciennes, 1833). Aquaculture Research **39**:1328-1338.

Fukuda, R., H. Ogawa, T. Nagata, and I. Koike. 1998. Direct determination of carbon and nitrogen contents of natural bacterial assemblages in marine environments. Appl. Environ. Microbiol. **64**:3352-3358.

Gaylard, S. 2014. Marine pollution within Spencer Gulf. Natural History of Spencer Gulf, Royal Society of South Australia Inc, Adelaide:378-391.

Glibert, P. M. 2017. Eutrophication, harmful algae and biodiversity—Challenging paradigms in a world of complex nutrient changes. Marine pollution bulletin **124**:591-606.

Green, R. H. 1979. Sampling design and statistical methods for environmental biologists. Wiley, New York.

Hertzfeld, M., J. Middleton, J. Andrewartha, J. Luick, and L. Wu. 2009. Chapter 1: Hydrodynamic modeling and observations of the tuna farming zone, Spencer Gulf. AquaFin CRC-Southern Bluefin Tuna Aquaculture Subprogram: Risk & Response-Understanding the Tuna Farming Environment:0000646-0000641.

Howarth, R. W. 2008. Coastal nitrogen pollution: a review of sources and trends globally and regionally. Harmful algae **8**:14-20.

Howarth, R. W., and R. Marino. 2006. Nitrogen as the limiting nutrient for eutrophication in coastal marine ecosystems: evolving views over three decades. Limnology and Oceanography **51**:364-376.

Lennon, G., D. Bowers, R. Nunes, B. Scott, M. Ali, J. Boyle, C. Wenju, M. Herzfeld, G. Johansson, and S. Nield. 1987. Gravity currents and the release of salt from an inverse estuary. Nature **327**:695.

Loo, M. G. K., and D. Giblot-Ducray. 2014. Yellowtail Kingfish (*Seriola lalandi*) Aquaculture Environmental Monitoring Program 2012/13 Report for Cleanseas Aquaculture Growout Pty Ltd, Boston Bay, South Australia: Licence Numbers AQ00015, AQ00139, AQ00235, FF00085 and FF00090. South Australian Research and Development Institute (Aquatic Sciences). Adelaide. SARDI Publication No. F2010/000207-5. SARDI Research Report Series No. 787.

Loo, M. G. K., and D. Giblot-Ducray. 2015. Southern Bluefin Tuna (*Thunnus maccoyii*) Aquaculture Environmental Monitoring Program 2014 Report: KIS Tuna Pty Ltd, Australian Fishing Enterprises Pty Ltd and SAMS Sea Farm Pty Ltd, Licence Number AQ00030. Report prepared for the Australian Southern Bluefin Tuna Industry Association Inc. South Australian Research and Development Institute (Aquatic Sciences). Adelaide. SARDI Publication No. F2009/000585-7. SARDI Research Report Series No. 822.

Loo, M. G. K., K. M. Ophel-Keller, and A. C. Cheshire. 2006. Final Report - Development of Novel Methodologies for Cost Effective Assessment of the Environmental Impact of Aquaculture. Aquafin CRC, Fisheries Research and Development Corporation and South Australian Research and Development Institute (Aquatic Sciences). Adelaide. SARDI Publication No. RD03/0036-4.

Loo, M. G. K., K. M. Ophel-Keller, A. C. McKay, Herdina, D. M. Hartley, S. Clarke, and A. Cheshire. 2010. Final Report - Development of rapid environmental assessment and monitoring techniques for application to finfish aquaculture in South Australia. Aquafin CRC, Fisheries Research and Development Corporation and South Australian Research and Development Institute (Aquatic Sciences). Adelaide. SARDI Publication Number F2010/000392-1, SARDI Research Report Series No. 477.

Madigan, S., S. Clarke, and K. Haskard. 2001. Southern Bluefin Tuna (*Thunnus maccoyii*) Environmental Monitoring Report: Licence-Based Monitoring Review and Recommendations. South Australian Research and Development Institute, Aquatic Sciences. Adelaide.

Marquis, E., N. Niquil, and C. Dupuy. 2011. Does the study of microzooplankton community size structure effectively define their dynamics? Investigation in the Bay of Biscay (France). Journal of Plankton Research **33**:1104-1118.

Menden-Deuer, S., and E. J. Lessard. 2000. Carbon to volume relationships for dinoflagellates, diatoms, and other protist plankton. Limnology and Oceanography **45**:569-579.

Middleton, J., M. Doubell, C. James, J. Luick, and P. Van Ruth. 2013. PIRSA Initiative II: Carrying Capacity of Spencer Gulf: Hydrodynamic and Biogeochemical Measurement Modelling and Performance Monitoring. Final report for the Fisheries Research and Development corporation. South Australian Research and Development Institute (Aquatic Sciences), Adelaide. SARDI Publication No. F2013/000311-1. SARDI Research Report Series No. 705.

Middleton, J. F., and M. Doubell. 2014. Carrying capacity for finfish aquaculture. Part I—Near-field semi-analytic solutions. Aquacultural engineering **62**:54-65.

Mobsby, D. 2018. Australian fisheries and aquaculture statistics 2017, Fisheries Research and Development Corporation project 2018-134. ABARES, Canberra.

Nixon, S. W. 1995. Coastal marine eutrophication: a definition, social causes, and future concerns. Ophelia **41**:199-219.

Nunes, R. A., and G. W. Lennon. 1987. Episodic stratification and gravity currents in a marine environment of modulated turbulence. Journal of Geophysical Research: Oceans **92**:5465-5480.

Nunes Vaz, R. A., G. W. Lennon, and D. G. Bowers. 1990. Physical behaviour of a large, negative or inverse estuary. Continental Shelf Research **10**:277-304.

Oke, P. R., P. Sakov, M. L. Cahill, J. R. Dunn, R. Fiedler, D. A. Griffin, J. V. Mansbridge, K. R. Ridgway, and A. Schiller. 2013. Towards a dynamically balanced eddy-resolving ocean reanalysis: BRAN3. Ocean Modelling **67**:52-70.

Paerl, H. W., L. M. Valdes, J. L. Pinckney, M. F. Piehler, J. Dyble, and P. H. Moisander. 2003. Phytoplankton photopigments as indicators of estuarine and coastal eutrophication. BioScience **53**:953-964.

Patten, N. L., P. D. van Ruth, and A. R. Rodriguez. 2018. Spatial variability in picophytoplankton, bacteria and viruses in waters of the Great Australian Bight (southern Australia). Deep Sea Research Part II: Topical Studies in Oceanography **157**:46-57.

Petrusevics, P. 1993. SST fronts in inverse estuaries, South Australia-indicators of reduced gulf-shlef exchange. Marine and Freshwater Research **44**:305-323.

Redfield, A. C. 1963. The influence of organisms on the composition of seawater. The sea **2**:26-77.

Saha, S., S. Moorthi, X. Wu, J. Wang, S. Nadiga, P. Tripp, D. Behringer, Y.-T. Hou, H.-y. Chuang, and M. Iredell. 2014. The NCEP climate forecast system version 2. Journal of Climate **27**:2185-2208.

Suthers, I., D. Rissik, and A. Richardson. 2019. Plankton: A guide to their ecology and monitoring for water quality. CSIRO publishing.

Tanner, J. E., D. Giblot-Ducray, and M. G. K. Loo. 2017. Temporal Analysis of Infaunal DNA Data from the Tuna and Finfish Environmental Monitoring Programs, 2005-2014. Report prepared for PIRSA Fisheries and Aquaculture. South Australian Research and Development Institute (Aquatic Sciences), Adelaide. SARDI Publication No. F2016/000392-1. SARDI Research Report Series No. 916.

Tanner, J. E., and J. K. Volkman. 2009. Aquafin CRC-FRDC Southern Bluefin Tuna Aquaculture Subprogram: risk and response: understanding the tuna farming environment. [West Beach, SA], Aquafin CRC; SARDI; FRDC.

Teixeira, C.E. 2010. The ocean circulation of Spencer Gulf: a numerical study. PhD thesis, University of New South Wales.

Thompson, R. O. 1983. Low-pass filters to suppress inertial and tidal frequencies. Journal of Physical Oceanography **13**:1077-1083.

Underwood, A. J. 1991. Beyond BACI: Experimental designs for detecting human environmental impacts on temporal variations in natural populations. Australian Journal of Marine and Freshwater Research **42**:569-587.

Underwood, A. J. 1994. On beyond BACI: sampling designs that might reliably detect environmental disturbances. Ecological Applications **4**:3-15.

Van Heukelem, L., and C. S. Thomas. 2001. Computer-assisted high-performance liquid chromatography method development with applications to the isolation and analysis of phytoplankton pigments. Journal of Chromatography **910**:31-49.

Van Meerssche, E., and J. L. Pinckney. 2019. Nutrient Loading Impacts on Estuarine Phytoplankton Size and Community Composition: Community-Based Indicators of Eutrophication. Estuaries and Coasts **42**:504-512.

Wiebe, P. H. 1988. Functional regression equations for zooplankton displacement volume, wet weight, dry weight, and carbon. A correction. Fisheries Bulletin **86**:833-835.

Wiebe, P. H., S. Boyd, and J. L. Cox. 1975. Relationship between zooplankton displacement volume, wet weight, dry weight and carbon. Fisheries Bulletin **73**:777-786.